THE MEDIA – AN INFLUENCE FOR GOOD OR EVIL?

CHIEF INSPECTOR PETER R. GRAHAM
OFFICER IN CHARGE
OPERATIONS MEDIA UNIT
SOUTH AUSTRALIA POLICE DEPARTMENT

KEYNOTE ADDRESS

Peter Graham, S.A. Police Prior to joining the South Australia Police Department, Chief Inspector Peter Graham worked as a radio broadcaster in the South-East of South Australia. His extensive policing career has seen him gain experience in numerous operational roles. His media experience has continued in the Police Department and he is now the Head of the Police Operations Media Unit. His voice may sound familiar, given his role as swimming commentator for the Sydney and Athens Olympics.

Who can forget the horrific images of the recent massacre at Beslan in North Ossetia? What parent could look dispassionately at the anguish on the weeping faces of those bereaved relatives and feel unable to identify with their pain? As grim as this whole saga has been it nevertheless provides an excellent exemplar of the influence of the media in shaping public opinion. Because of the global media exposure, the world at large, including the Arabic world, has now roundly condemned the outrage perpetrated by the Chechens. And make no mistake it is an outrage by any measure of such things. But pause and consider another side to this story, a side which has been largely hidden due to media censorship. The low media profile on all of this prior to the Beslan attack can be easily demonstrated - how many people in the West can point to a map and accurately place the Caucasian lands of Chechnya, North and South Ossetia, Ingushetia and Dagestan?

The Chechens allege that in recent years Russia has perpetrated a multitude of atrocities on the Chechen people, and included in these are the deaths of 42,000 Chechen children of school age. Tucked away in a rather obscure section of Time Magazine was a report of a Chechen woman soldier who was killed by Russian soldiers. So what? – war is war, one might think. But to kill her by tying each of her legs to a different motor vehicle and driving off in opposite directions adds a gruesome, sadistic dimension to what has been going on largely behind the scenes. Despite this atrocity, and no doubt many others like it perpetrated by the Russian Army, the Chechens have now lost any vestige of international empathy. The Beslan attack, with its graphic front-seat, real-time exposure to world media, has blown away any credibility or justification that the Chechen cause might have. The old truism is certainly true in this case, "people's perception becomes their reality". Across the world, the Chechens are now largely perceived as pariahs and this Beslan incident has also been disastrous for them, at least from the point of view of the promotion of their cause.

No doubt, as the Beslan saga unfolds into the longer term, we will see yet another example showing that if there is asymmetry in reporting the different points of view on issues, distorted perspectives will result, power-brokers will align themselves unfairly and ultimately distorted, unfair strategies will be adopted. What a difference a free press could have made!

It should go without saying that there ought to be a free press. Nobel Prize laureate Amartya Sen asserts that "No substantial famine has ever occurred in any country with a relatively free press". The world-renowned professor of economics argues that the independent media also provide a voice to the neglected and disadvantaged while simultaneously preventing governments from insulating themselves from public criticism.

The suppression of the media and the 30 million death toll by starvation during the Mao Tse Tung's early -1960s "Great Leap Forward" programme testify to the veracity of Amartya Sen's observation, as do recent events in North Korea.

The media can also be most helpful when it comes to emergency management applications. The summation of live footage from individual media outlets is useful to emergency managers in developing an overall picture of what is happening. Also of vital importance is the role that the media has in enhancing public safety by being able to readily relay information, in real-time, to the community during times of crisis.

So far so good, now for some words of caution. Whilst we would want to see the media as conduits of truth, there is a pragmatism that needs to be taken into account. The media is also in the business of staying in business, and much of that has to do with ratings and sensational reporting. The media
outlet with a ho-hum report is no match for the one with the sensational story.

Media behaviour needs to be understood. When something sensational happens the consequent media behaviour is predictable and it has identifiable phases:

Phase 1: ***Information Gathering (the "Mayhem" phase)*** - Enormous resources are deployed for the urgent collection and publication of any and all information about the incident. Speculation may be substituted for fact where no information is provided. (For example, after the Whyalla Airlines crash, relatives of the deceased hid for three days in the Whyalla Police Station for no other reason than to escape media harassment. After the Port Arthur shooting, some journalists fronted up to Airline booking counters on the mainland, posing as relatives of the deceased in order to secure seats on aeroplanes going to Hobart).

Phase 2: ***Analysis (the "Mastermind" phase)*** - Journalists, with the help of "experts", will look for motives, political and social causes and background information; they may try to explain or anticipate response tactics and predict outcomes.

Phase 3: ***Blame Attribution (the "Manhunt" phase)*** - The media will try to determine who is to blame for the incident, for anything that goes wrong, and in particular for any human suffering which occurs. (For example after the Whyalla Airlines crash, the media laundered accounts of the deceased pilot's relationship with his boss and how the pilot has been required to work when tired).

Another model, especially applicable to Police murder investigations, sees three sequential phases through which the media move:

- Cooperation (initially) The story has broken and there is plenty of material to go around, so everyone will be satisfied that they have the story and can placate their editors with plenty of detail.

- Competition (for the best scoop) The desire for a new angle. Media outlets ring person X, *claiming* that person X's boss Y has said that it is O.K. for X to discuss details with the media.

- Controversy (finding an issue upon which to build a story) Starved of any new information, if reporters can't get information, they might start looking for an internal controversy.

Needless to say the behaviour of the media has relevance for earthquake engineers. Any earthquake engineer who believes that the media has no part to play in his/her

profession is deceived. After an earthquake, questions will be asked and people will be blamed. Fore-warned is fore-armed.

Some helpful pointers for earthquake engineers when dealing with the media are:

1. Have an in-depth crisis communications plan that includes dealing with the media, the community and your employees (if applicable).

2. Deal with the issue head-on. Do not hide out.

3. Respond to reporters' questions promptly. They expect a return call or an on-site interview within 10 minutes of the request.

4. Never tell lies.

5. Never go off the record. Tell a reporter only what you want to see on the front page of the local paper.

6. Do not speculate, nor talk outside of your area of expertise. Defer to those who do have the expertise.

7. Don't use humour. Humour is contextual and has the potential to cause offence and distress.

8. If you are being interviewed, remember the interviewer's first name and use it throughout the interview

9. Don't rush your answers. Don't feel forced to talk quickly. Make sure the brain and mouth are synchronised.

10. If possible have a strategy by which you can lure the media into a "safe" area that you are comfortable to talk about.

I finish by posing again the question in the title of my address. The media – an influence for good or evil? The truth is that they can be both good and evil, depending on the circumstances. Be that as it may, they are nevertheless a reality of the world we live in and from time to time we may find ourselves under their spotlight. It is helpful to know the sort of things one might expect from them.

NEW ZEALAND ARRANGEMENTS FOR MONITORING, RESEARCH AND MITIGATION FOR GEOLOGICAL HAZARDS

DR. HUGH COWAN
NATURAL HAZARDS GROUP

KEYNOTE ADDRESS

Dr Hugh Cowan, Manager, GeoHazards Monitoring, Natural Hazards Group. Hugh is manager of the GeoNet Project - a 10-year programme to gradually upgrade the equipment and systems that monitor earthquakes, volcanic eruptions and land deformation in New Zealand. The $50 million project, core funded by the Earthquake Commsssion, is one of the biggest earth science projects in New Zealand in the past 30 years. Hugh has degrees in geology, engineering geology, and geophysics from Victoria and Canterbury Universities. He has worked in Scandinavia, the Middle East and Latin America. Before he returned to New Zealand in 1998, he was an independent natural hazards consultant in Panama City.

Popular conceptions of New Zealand are generally synonymous with benevolent Nature - lush, sparsely populated lands of physical contrast and natural beauty, endowed with a temperate climate and benign fauna. Of the 4 million inhabitants and 1 million visitors to New Zealand each year, relatively few appreciate the scale of the forces that created this environment and the destructive power released periodically in earthquakes and volcanic eruptions at the Pacific-Australian plate boundary. Historical records and scientific research show clearly however, the level of geological hazard is far higher than the past 60 years would indicate.

Few alive today have personal experience of damage or loss to geological hazards, but a variety of tools to mitigate vulnerability and natural hazard risk has evolved in New Zealand in response to earlier historical events and international practices. These include a regulatory framework for land use and building, incorporating codes and standards, plus an instrument of social policy - the Earthquake Commission - using the insurance model, which provides cover for losses to residential property caused by earthquake, volcanic eruption, tsunami, landslip or geothermal subsidence. Recently enacted civil defence legislation places greater emphasis on accountability for risk management or avoidance at all levels of community decision-making. These new arrangements extend and formalise, among other things, the successful voluntary efforts undertaken by engineering lifelines groups to reduce community vulnerability.

Recognising that the risk management process has no basis without the ability to detect hazards and evaluate trends, a major renewal of New Zealand's geological hazard monitoring system (GeoNet) began in 2001. The purpose of GeoNet is to provide more accurate and rapid information on earthquakes, volcanic unrest, slow earth deformation and landslides, to inform emergency management and to guide science and engineering research on natural hazard risk, leading to long-term incremental reductions in the exposure to risk.

The challenge overall is to optimize the different countervailing measures described above to ensure as the New Zealand economy and population grows, a wide range of agencies can respond effectively to future natural hazard events, to minimise damage, loss of life, and the cost of recovery. The presentation will illustrate the scope of this work as well as highlighting some of the gaps in understanding of natural hazard risk and organisational challenges that lie ahead.

TOWARDS A NATIONAL PICTURE OF EARTHQUAKE RISK IN AUSTRALIA

JOHN F. SCHNEIDER
GEOSCIENCE AUSTRALIA

KEYNOTE ADDRESS

John F. Schneider is the Group Leader of the Risk Research Group at Geoscience Australia. This Group, which comprises hazard scientists, engineers, mathematicians, social scientists and economists, is developing sudden-impact risk models for a wide range of hazards in Australia. John's research expertise is in earthquake hazard and risk modelling. Prior to his arrival in Australia in 2000, John was Chief Scientist at Aon-Impact Forecasting, a risk modelling company based in Chicago, Illinois, USA (1995 to 2000) and Project Manager for Earthquake Hazard Research at the Electric Power Research Institute in Palo Alto, California, USA (1987 to 1994).

ABSTRACT:

This paper explores the issues associated with developing a new national picture of earthquake risk in Australia. Current research efforts are focussed on developing a comprehensive view of risk by combining information about earthquake hazard, vulnerability and exposure. Advances in hazard analysis are shifting the focus from traditional earthquake monitoring toward neotectonics research and ground motion wave propagation modelling. Vulnerability analysis has shifted from subjective estimates of damage using the Modified Mercalli Intensity scale to complex combinations of models which capture physical, social and economic aspects of earthquake (and other natural hazard) impact. Exposure databases are also being developed so that earthquake risk can be mapped nationally in Australia. In combination, this work will ultimately allow earthquake risk to be objectively measured across Australia as well as to be compared to the risks posed by other sudden-impact natural hazards. This capability will provide the basis for improved decision making for a wide range of applications from insurance to building codes and from government to corporate risk management.

1. INTRODUCTION:

In Australia, damaging floods, tropical cyclones and bushfires are fairly common and therefore appreciated as risks by the public and government officials. Damaging earthquakes, on the other hand, are rare and therefore do not get much attention in common emergency management practice. Even earthquake hazard/risk experts do not really understand the probability or potential impact of a major earthquake in Australia. Increasing this understanding requires some changes and advances in the way we research and analyse this risk.

The recent review of natural disaster risk management arrangements in Australia by the Council of Australian Governments (2002) points to the need to develop better strategies for mitigating the effects of sudden-impact natural hazards. It is difficult to place priorities on mitigation strategies because risks from different natural hazards are not well quantified, and therefore can not readily be compared. The report recommends that emphasis be placed on developing risk assessment methods, models and data as a means of improving our ability to make appropriate risk management decisions. Other drivers, such as critical infrastructure protection and global warming issues, are also bringing about a significant shift in mind set of emergency managers from a traditional focus on response and recovery, towards a demand for planning and preparation. Thus, in response to this new demand for better understanding of multi-hazard risk on a national scale, we have an opportunity and obligation to improve our understanding of earthquake risk in Australia.

To do this, we need to rethink the manner in which we measure earthquake risk. Figure 1 shows a risk analysis flow chart which is appropriate for earthquakes as well as a wide range of other hazards. This flow chart complements the Australia-New Zealand Risk Management Standard (Standards Australia, 1999) by providing a detailed conceptual approach to analysing risk. Broadly speaking, this flow chart addresses the relationship between hazard, vulnerability and exposure (or elements at risk), which combine to form a measure of risk (Crichton, 1999). Historically the focus has been on monitoring earthquakes and developing catalogues of earthquake magnitudes and locations. This effort provides some information for the upper left-hand box of the flow chart, which in turn provides some constraints on the "event occurrence" box in the lower left corner, albeit of fairly limited value. Moving to the right in the flow chart, our knowledge becomes even more limited and our models are correspondingly more primitive. As an example, our knowledge of ground motion in Australia is so poor that the only ground motion attenuation model that has been published for Australian conditions is based on Mercalli Intensity (Gaull et al, 1990). Moving to physical impact or damage, while we can model the response of individual structures to known earthquake shaking input, our ability to model the potential damage to the entire physical infrastructure is poor. Our models, to the extent that they do exist, rely almost exclusively on data and models derived from other regions of the world.

While the hazard and physical damage components of an earthquake risk model are unique to earthquake, defining the elements at risk and measuring the social and economic impact of an earthquake are common to all sudden-impact hazards. In these areas we can take advantage of work being done in a multi-hazard risk framework in

order to improve our understanding of earthquake risk. This paper explores the areas of research that represent significant opportunities to advance our understanding of earthquake risk in Australia. Examples are taken largely from work currently being undertaken at Geoscience Australia (GA). The sections are divided into the three main components of a risk model: hazard, vulnerability and exposure (or elements at risk).

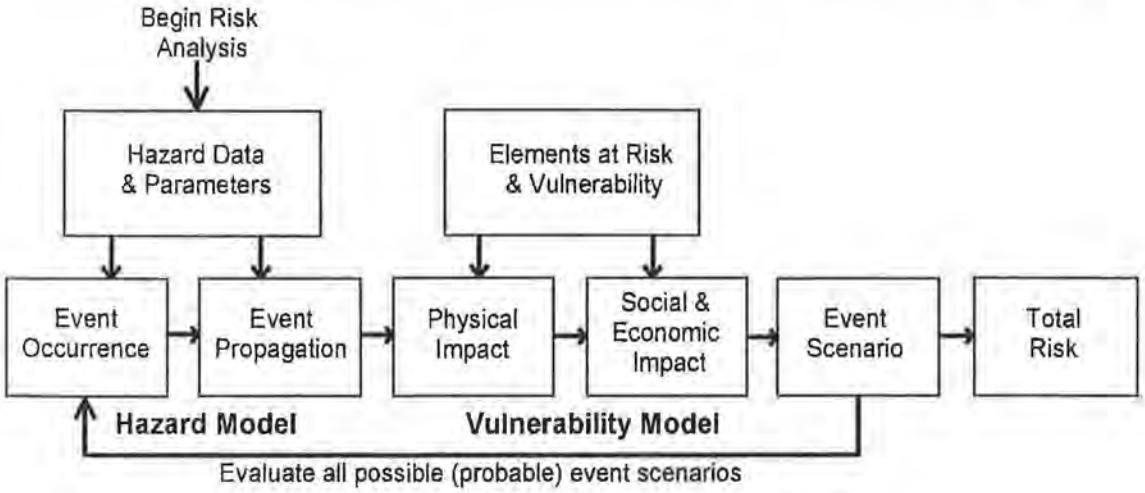

Figure 1. Computational risk assessment framework (from Schneider et al, 2003a).

2. HAZARD MODEL:

2.1. Event occurrence. In most stable continental regions, such as Australia, the relationship between seismicity, faults and present day tectonics is poorly understood. The lack of a definitive geophysical or geological model, at any scale, describing seismicity imposes significant limitations upon the methods that can be employed to estimate earthquake hazard, and on the certainty of our estimates of earthquake hazard. Present-day estimates of future patterns in seismicity are based on statistical analyses of the last 100 years of instrumentally recorded earthquake data. This is a very short and sparse dataset, particularly when large earthquakes (in the magnitude range 6.8 - 7.0) might occur only once in a century across the entirety of Australia. Furthermore, the fundamental assumption that future significant events will occur in regions characterised by concentrations of historic seismicity has not been rigorously tested.

A variety of geological and geophysical tools is being developed to overcome the limitations imposed by the short historical record of earthquakes. As summarised by Schneider et al (2003b), the following tools are being employed in several test-areas in Australia:

- Evaluation of stress in the earth's crust from studies of the movements of past earthquake faults (called "focal mechanisms") (Clark and Leonard, 2003);
- Evaluation of ongoing deformation of the earth's crust using GPS satellite receivers (Featherstone et al, 2003);
- Mapping earthquake locations and faults using high-precision seismic arrays;

- Extending fault mapping/imaging to the third dimension using geophysical data (aeromagnetics, seismic signals, and ground-penetrating radar); and
- Trenching investigations of fault scarps to reveal information regarding prehistoric earthquake events (Clark et al, 2001; Clark and McCue, 2003; Clark et al, 2004).
- Modelling the relationship between stress and strain in the earth's crust to explain the overall rate of earthquake activity in Australia (Burbidge, 2004).

2.2. Event Propagation. For earthquakes, event propagation can be divided into two parts: 1) ground motion attenuation, which represents wave propagation through the earth's crust; and 2) site response, which represents regolith or soil amplification effects at the near surface.

The correct choice of attenuation model is vital in order to reduce the uncertainty in future risk assessments. Very little is known about the appropriate attenuation model (or models) for Australian conditions. One model, Gaull et al (1990), was developed for Australian conditions, but is based entirely on seismic intensity data (Modified Mercalli), which are derived from personal perceptions of shaking and damage. As part of this study, a conversion factor was developed for estimating peak ground acceleration (PGA), but this conversion is fraught with uncertainty. Therefore, earthquake risk assessments in Australia typically adopt attenuation models from other stable continental regions such as eastern North America. For example, in GA's earthquake risk assessment of Newcastle and Lake Macquarie the Toro et al (1997) attenuation model was used (Dhu and Jones, 2002). However, there has been very little analysis undertaken to suggest that the Toro et al (1997) model is any more or less applicable to Australian conditions than other models developed for stable continental regions. Moreover, there has been conjecture that attenuation in some parts of Australia resembles that of active tectonic regions and may be better described by models such as Sadigh et al (1997), which was developed primarily from earthquake recordings in western North America, especially California.

Consequently, current work at GA is focussing on using Australian earthquake ground motion recordings to reduce the uncertainty in attenuation models. From an analysis of close-in ground motion recordings of the Burakin swarm, Allen et al (2004) find that the intrinsic Q of the crust in WA is as high or higher than crustal Q in cratonic North America. If so, then in SW Australia at least, further analysis should result in an Australian-based ground motion attenuation model with ground motion decay rates similar to models developed for Eastern North America.

Irrespective of the choice of attenuation model, there is a need to incorporate detailed local geology into any earthquake risk assessment. The presence of regolith (i.e. soils, geological sediments and weathered rock material) can dramatically increase the amount of ground shaking experienced during an earthquake. The effect of regolith is usually incorporated into earthquake risk assessments through a site response model consisting of detailed geotechnical models and amplification factors. These amplification factors are applied to the rock ground motion estimated from the attenuation model to determine the ground

shaking experienced at the surface. Dhu et al (2002) have developed earthquake site amplification factors for Newcastle-Lake Macquarie, and factors are under development for Perth. Further, GA is developing a site classification model and site amplification factors for major urban centres throughout Australia. A preliminary model will be completed by mid 2005. Beyond this, significant effort is required to gather detailed geological and geotechnical data and to measure ground response in order to realistically capture regolith response for input to risk maps and ultimately for input to the Australian Building code.

2.3. **Changing the Way we Monitor Earthquakes.** Our ability to make significant improvements to the estimation of earthquake hazard in Australia is highly dependent upon the availability of high-quality earthquake ground motion recordings. The convergence in research requirements and technology suggest that we now have an opportunity to implement a new model of urban earthquake monitoring which will enable us to make a quantum improvement in the recording of seismic data in urban centres. Specifically, we should consider deploying a new Joint Urban Monitoring Program (JUMP) in Australian cities that allows us to capture both low- and high-amplitude ground motion data across a wide frequency band. The frequencies and dynamic range should be sufficient to capture 6 to 7 orders of magnitude in dynamic range at a bandwidth of 0 to 50 Hz in order to accurately record information from all earthquakes ranging from ambient noise to strong motion. Low cost instruments meeting these basic requirements are now available. As a starting point, a dozen or so instruments could be deployed in a key urban area to monitor activity for 6 months for proof of concept, followed by consideration for similar arrays in other urban areas.

3. VULNERABILITY AND EXPOSURE

From risk a modelling point of view, vulnerability represents the relationship between hazard and impact. As shown in Figure 1, risk is measured as a combination of all possible impacts and their probabilities. While there is no one definition of vulnerability, it generally refers to how people, infrastructure and the economy are affected by a hazard event. We divide the vulnerability factors into three main areas: physical, social and economic.

3.1. **Building Damage.** The Modified Mercalli Intensity (MMI) has been used extensively to describe damage from earthquakes in Australia and New Zealand (Gaull, 1990; Dowrick, 1996). Over the past decade, earthquake risk models have begun to incorporate engineering-based methods to develop objective relationships between the ground motion input to a structure and the resulting physical damage. At GA the method we have been developing to estimate potential building damage is based on the earthquake scenario computational program "HAZUS" (National Institute of Building Sciences, 1999). The HAZUS methodology makes use of the capacity spectrum method to first estimate damage, and then to estimate cost based on repair and replacement values as a function of the predicted damage state.

The problem we face is that the damage parameter values in the HAZUS methodology are based primarily on U.S. construction standards typically associated with high-seismicity regions. These parameters require modification for application to Australian conditions. The lack of empirical data on building performance makes this area of model development a particular challenge. Schneider et al (2003b) show that the uncertainty in building damage parameters is in fact one of the largest uncertainties in estimating earthquake risk. Recent progress has been made in using available damage data from the Newcastle earthquake, including the seismic intensity data, to calibrate damage curves that are tied to spectral acceleration (e.g., Edwards et al, 2004).

3.2. **Critical infrastructure.** Critical infrastructure is defined as those physical facilities, supply chains, information technologies and communication networks which, if destroyed, degraded or rendered unavailable for an extended period, would significantly impact on the social or economic well-being of the nation. GA is engaged in a pilot project with the New South Wales government to identify and model the risk of extreme event interruption to the electricity supply. The objective will be determine the direct effects of loss of supply to the community, as well as the indirect social and economic impacts, interdependencies and cascading effects across a range of other infrastructure systems and service providers. GA is also beginning work on a Critical Infrastructure Protection Modelling and Analysis Project managed by the Attorney General's Department. The purpose of this project is to simulate through computer modelling the interdependencies of a wide range of infrastructure systems (e.g., banking and finance, communication, energy) and their vulnerabilities to points and mechanisms of failure. In theory, whether the failure is caused by an earthquake, a flood, or a terrorist attack, the system response should follow certain rules that enable one to predict its overall behaviour, such as recovery time and economic impact.

3.3. **Social and Economic Vulnerability.** Economic losses from natural disasters can be broadly classified as tangible and intangible and sub-categorised into direct and indirect losses, (e.g., National Institute of Building Standards, 2000). Tangible direct losses are losses such as physical damage to buildings, infrastructure, contents, and vehicles; whereas tangible indirect losses represent factors such as the associated disruption to businesses, transport and utility networks. Intangible direct losses include death and injury, and loss of memorabilia; and intangible direct losses are factors such as household disruption and health effects. GA is developing models for both direct and indirect economic losses. For instance, direct losses associated with the disaster recovery process can be captured by evaluating loss of business income and household disruption such as building repair time (Milne, 2004). Indirect losses, such as the effect of damaged buildings from an earthquake, can also be modelled as an economic shock to capital stock. Using a model developed by Monash University, GA is assessing the indirect flow-on effects of building damage from a major earthquake in Perth on a range of economic sectors (Witwer et al, 2004).

How people cope in the event of a natural hazard is often related to the effects of personal injury and damage to dwellings. Other factors include access to community support and health. This network of factors is referred to as social vulnerability. Dwyer et al (2004) investigated how factors such as income, home insurance and home ownership might affect one's ability to recover from an earthquake or other natural hazard event. The study found that personal injury and residence damage are the most significant factors in defining the need to recover; while factors such as age and financial status are most critical to recovery time. The methodology has been applied to a case study area and is now being extended to 46 Local Government Areas in the Perth metropolitan area.

4. EXPOSURE OR ELEMENTS AT RISK

The number of people, buildings and infrastructure within an area influences the total risk. This exposure data is essential to any risk assessment. Analysis of risk to a community requires the development of extensive data-sets that define the most vulnerable components of our communities. Key databases of interest are the following:

- Building construction classifications and distributions.
- Building codes, construction practices and costs.
- Critical infrastructure (roads, water, power, sewerage, emergency facilities, hospitals, etc...).
- Cadastre (land boundaries and ownership).
- Census data (population distribution, income, and other statistics such as age, occupation, disability, education).
- Economic data (business sectors, industrial production, exports, imports, etc).
- Emergency management arrangements for disaster response and recovery).

These data provide the basis for vulnerability assessments of earthquakes as well as floods, severe winds, bushfires and terrorist attack. These data provide the input to any analysis of the potential impact of an event. In order to conduct risk assessments on a national scale, exposure databases need to be developed beginning at the local level and integrated at the State/Territory and Commonwealth level, in order to assure uniformity in the assessment process.

The development of comprehensive exposure databases on an urban, regional or national scale is an enormous task. Fortunately, there are simpler means to defining exposure that can be exploited to assess risk on a regional or national scale. Techniques are being developed using remotely sensed satellite imagery and census data to develop proxy exposure data. The technique can be benchmarked where detailed local building/infrastructure data has already been collected at a local scale. GA is in the process of developing a proxy exposure database of major urban areas in Australia. In the coming year, GA will be developing a national picture of natural hazard risk combining this information with vulnerability curves for residential structures and hazard models for a range of sudden-impact hazards.

5. CONCLUSIONS:

This paper explores the issues associated with developing a new national picture of earthquake risk in Australia. Current research efforts are focussed on developing a comprehensive view of risk by combining information about hazard, vulnerability and exposure. This work will ultimately provide information that can be used to objectively compare earthquake risk across Australia and to compare earthquake risk to the risks posed by other sudden-impact natural hazards. This capability will provide the basis for improved decision making for a wide range of applications from insurance to building codes and from government to corporate risk management.

REFERENCES:

Allen, T, Dhu, T., Cummins, P., and Schneider, J. (2004) Some empirical relations for attenuation of ground-motion spectral amplitudes in south-western Western Australia, Proceedings: Annual meeting of the Australian Earthquake Engineering Society, Mt. Gambier, VIC, Australia, Nov. 2004.

Burbidge, D. (2004) Thin plate neotectonic models of the Australian plate, J. Geophys. Res. (in proof), vol 109, p. xx.

Clark D J and Leonard M, (2003) Principal stress orientations from multiple focal plane solutions: new insight in to the Australian intraplate stress field: eds Hillis, R.R. & Muller, D., Evolution and dynamics of the Australian Plate, G.S.Australia and G.S.America, Joint Special Publication, v. 22, p. 91-105.

Clark D.J. and McCue K., (2003) Australian palaeoseismology: towards a better basis for seismic hazard estimation: Annales of Geophysics, v. 46, p. 1087-1105.

Clark D.J., Cupper M., Sandiford M., and Kiernan K., (2004) Style and timing of late Quaternary faulting on the Lake Edgar Fault, southwest Tasmania, Australia: implications for hazard assessment in intracratonic areas: Geological Society of America Special Publication on Paleoseismology, v. in review.

Clark, D J., Dentith, M., Wyrwoll, K H., Featherstone, W., Yanchou, L. and Dent, V. (2001) Palaeoseismological investigations on the Hyden Fault scarp, Western Australia: towards a Better Understanding of the Recurrence Rate of Large Australian Intraplate Earthquakes. ILP2001 Conference Kaikoura New Zealand, p.39-40.

Council of Australian Governments (COAG) (2002) Natural disasters in Australia: Reforming mitigation, relief and recovery arrangements. Commonwealth Department of Transport and Regional Services, Canberra, Australia.

Crichton, J. (1999) The risk triangle, in Ingleton, J. (ed.) Natural Disaster Management, a presentation to commemorate the International Decade for Natural Disaster Reduction (IDNDR). Tudor Rose: UK.

Dhu, T and Jones, T. (eds.) (2002) Earthquake risk in Newcastle and Lake Macquarie; Geoscience Australia Record 2002/15. Canberra: Geoscience Australia.

Dwyer, A., Zoppou, C., Nielsen, O., Day, S., and Roberts, S. (2004) Quantifying social vulnerability: A methodology for identifying those at risk to natural hazards, Australian Government: Geoscience Australia, Record 2004/14.

Edwards, M., Robinson, D., McAneney, K., and Schneider, J. (2004) Vulnerability of residential structures in Australia, Proceedings: Thirteenth World Conference on Earthquake Engineering, Paper No. 2985, Vancouver, B.C., Canada, Aug. 2004.

Featherstone, W.E., Penna, N.T., Leonard, M., Clark, D.J., Dawson, J., Dentith, M.C., Darby, D. & McCarthy, R. (2004) GPS-geodetic deformation monitoring of the southwest seismic zone of Western Australia: epoch one. Journal of the Royal Society of Western Australia, in press.

Gaull, B A., Michael-Leiba, M O., and Rynn, J M W. (1990) Probabilistic earthquake risk maps: Australian Journal of Earth Sciences, Vol 37, p. 169-187.

Milne, M. (2004) Modeling economic impacts of natural hazards on Australian urban communities. Proceedings of the Annual Australian Agriculture Society, Melbourne, VIC, Australia, February 2004.

National Institute of Building Science (1999) HAZUS technical manual, Federal Emergency Management Agency, United States Government, Washington D.C., USA.

Sadigh, K., Chang, C.-Y., Egan, J A., Makdisi, F., and Youngs, R R. (1997) Attenuation relationships for shallow crustal earthquakes based on California strong motion data. Seismological Research Letters, Vol 68(1), p.180-189.

Schneider J., Robinson D., Clark D., Dhu T. & Edwards M. (2003a) Earthquake risk in Australia: How well do we understand it? Proceedings: Catastrophic Risks and Insurability, Aon Re Hazards & Capital Risk Management Conference Series, Gold Coast, QLD, Australia, Aug 2003, p. 37-62.

Schneider, J., Hayne, M., Dwyer, A. (2003b) Natural hazard risk models: Decision-support tools for disaster management, Proceedings: 2003 Australian Disasters Conference, Canberra, Australia, Sept. 2003.

Standards Australia (1999). Australia New Zealand Standard AS/NZS 4360:1999 Risk Management Standards Australia, Homebush, Standards New Zealand, Wellington.

Toro, G R., Abrahamson, N A., and Schneider, J F. (1997) Model of strong ground motions from earthquakes in Central and Eastern North America: Best estimates and uncertainties. Seismological Research Letters, Vol 68(1), p.41-57.

Wittwer, G., Mullaly, D. and Milne, M, (2004) Modelling the economic impacts of a significant earthquake in the Perth Metropolitan area, prepared for Geoscience Australia, Monash University, Melbourne.

REVISION OF THE PARAMETERS OF THE 1972 TEMORA EARTHQUAKE

CVETAN SINADINOVSKI
GEOSCIENCE AUSTRALIA

AUTHORS:

Cvetan Sinadinovski, PhD in Geophysics – Flinders University of South Australia, has worked for many years as a visiting fellow in USA and Europe, and as a software specialist in Sydney and Adelaide. Currently employed as a Seismologist in Geoscience Australia in Canberra. Member of AIG, Association of Physicists of Macedonia and AEES.

ABSTRACT

Geoscience Australia's (GA) Earthquake Hazard and Neotectonics (EHN) group recently re-evaluated the 1972 Temora earthquake which occurred on 25th of February. The seismological literature was in poor agreement regarding the size of this event, with different authors estimating its magnitude to be as low as 4 and as high as 5.1 on the Richter scale.

We collected the available Australian seismograms of the event and analysed them in detail. Using our current program for magnitude and location calculation we revised the local magnitude of the 1972 Temora event to 4.4 and compared the solution with other published information. Continuing improvement of Australia's earthquake catalogue in this manner will lead to better estimates of earthquake recurrence and hence of seismic hazard. Over the next few years EHN hopes to review a large number of events in GA's earthquake catalogue using improved velocity models and location algorithms in a similar attempt to improve hypocenter and magnitude estimates.

1. INTRODUCTION

Studies of earthquake hazard and seismic risk depend profoundly on information from past damaging earthquakes and their geological and geophysical settings. In regions with relatively low seismicity like Australia, it is very important to understand the processes which determine the seismogenic zones and the frequency of occurrence of events with larger magnitudes, because even one large event can make a big difference on the probabilistic hazard estimates.

We have revised one such event - the 1972 Temora earthquake which occurred on 25th of February and is listed as a moderate size earthquake with magnitude estimates varying according to different authors between 4 and 5.1 on the Richter scale (Drake, 1974; Denham *et al.*, 1985; AGSO Earthquake Database 2003). Available seismograms were collected from the archives and analysed in details using GA's current software and compared with the solutions which appeared in the Bulletin of the International Seismological Centre (ISC Bulletin, 1972).

According to Drake (1974), the ground motion at Riverview College Observatory caused by earthquakes in New South Wales between 1909 and 1973 has been measured and estimated of the Wood-Anderson instruments. The epicentre and the origin times of the Temora 1972 event were based on the calculation at the Australian National University, and in his table he associated a magnitude M_L of 4.0 using the Richter formula for Southern California.

In the work of Denham *et al.* (1985), the Temora 1972 event was examined in comparison to the 1982 Wyalong earthquakes which occurred about 37km from the 1972 epicentre. A magnitude of $M_L \sim 4.5$ was assigned by the authors, while the first motion indicated a strike-slip faulting mechanism related with almost north-south compressive stresses in the crust.

We also thoroughly searched the newspaper records for any mentioning of the event; no explicit reference could be found in "Canberra Times", "Sydney Morning Herald", "Tumut" and "Adelong Advertiser", and no isoseismal map was compiled at the time, as would be expected for an earthquake of higher magnitude.

2. SEISMOGRAMS

For the purpose of our analysis, we retrieved the paper seismograms from the regional stations in Canberra (CAN), Riverview (RIV), Toolangi (TOO), Adelaide (ADE), and Warramunga (WRA). Most of the records are such that the S-phase is very hard to identify. The short-period records of the Canberra stations are clipped which made them unusable for magnitude calculation.

Canberra was the closest station and its short-period record was very faint and practically unreadable. The only information we used was the P-arrival and we detected that the clock was about 40 seconds fast.

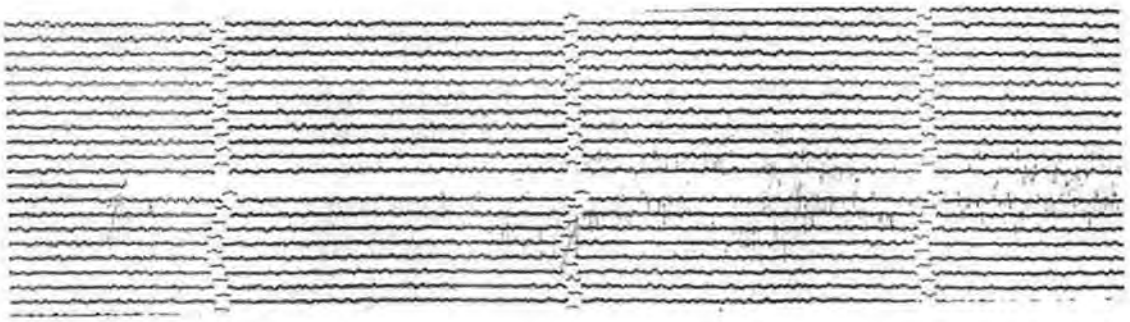

Fig 1: Canberra short-period seismogram of the 1972 Temora quake (Z - component)

We used this record from the Canberra long-period instrument to read the S-arrival, otherwise only available formula for local magnitude calculation was for the short-period seismographs.

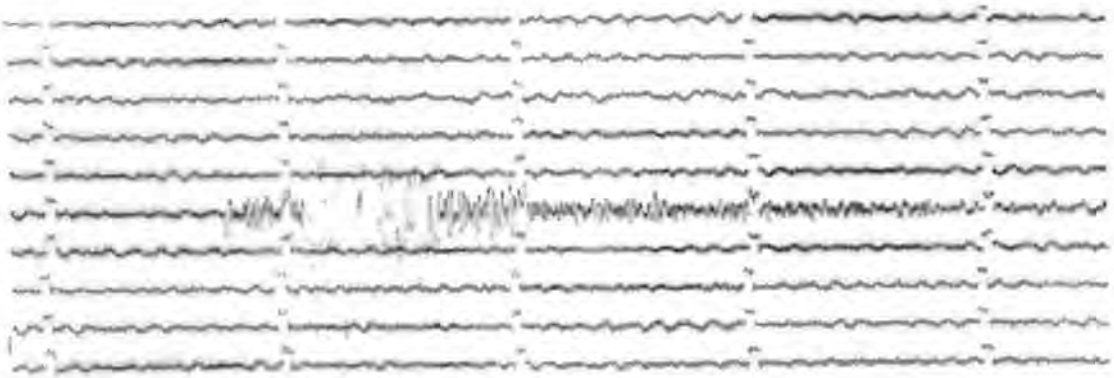

Fig 2: Canberra long-period seismogram of the 1972 Temora quake (Z-component)

Phases on the Riverview seismogram were also hard to be identified, specially the S-wave. The magnitude estimate based on the S-P difference could vary between 4 and 5 depending on the reading of the S-arrival.

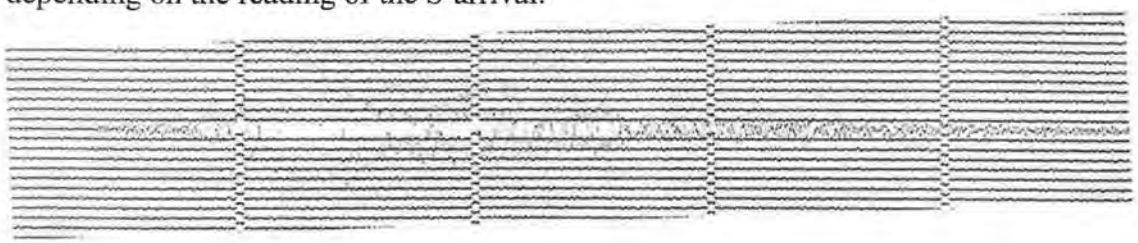

Fig 3: Riverview short-period seismogram of the 1972 Temora quake (N-component)

This long-period component helped us to identify the S-arrival and that time is close to the reading which appeared in the ISC bulletin.

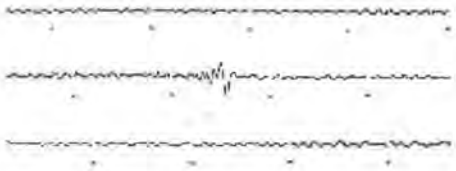

Fig 4: Riverview long-period seismogram of the 1972 Temora quake (Z-component)

Toolangi was the southern station which helped to constrain the epicentral solution in the N-S direction. With the magnification of the World Wide Standardised Seismograph Network it did not record well the amplitudes of the S-waves and was very hard to estimate whether the upper and lower peaks of our measurements really belonged to one single oscillation.

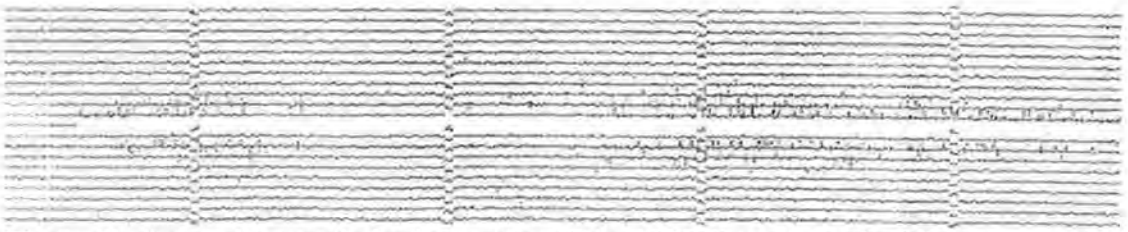

Fig 5: Toolangi short-period seismogram of the 1972 Temora quake (E-component)

The three-component seismograms at the Adelaide station are shown on the figure below. The instrument was more than 500km away from the epicentre and the observations and calculations should be viewed in that perspective.

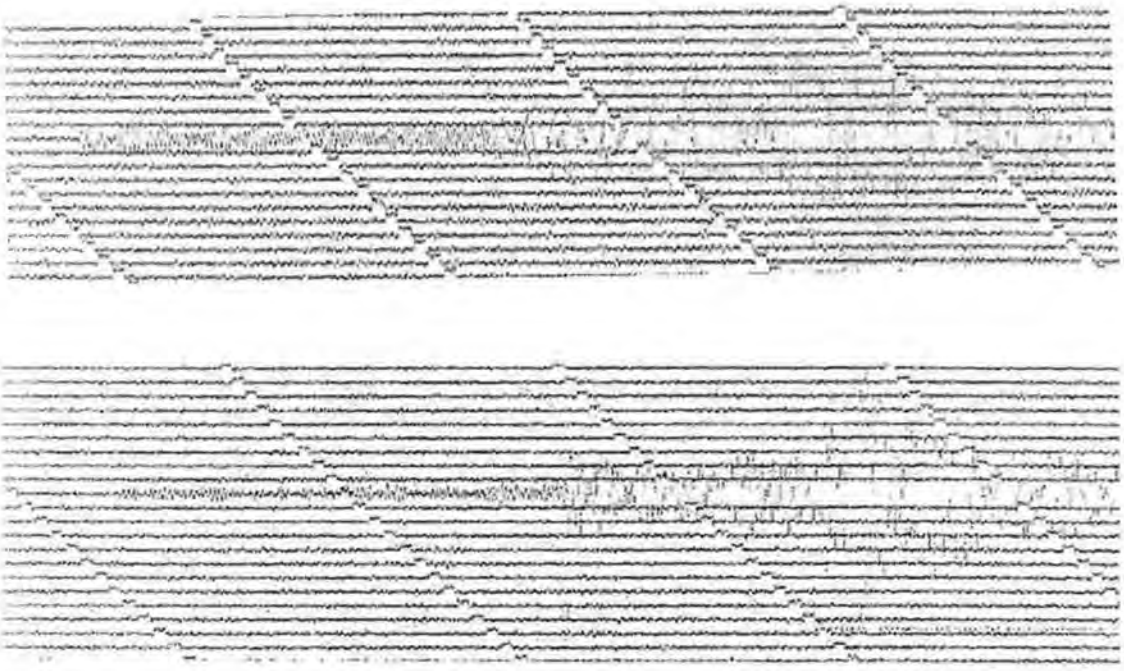

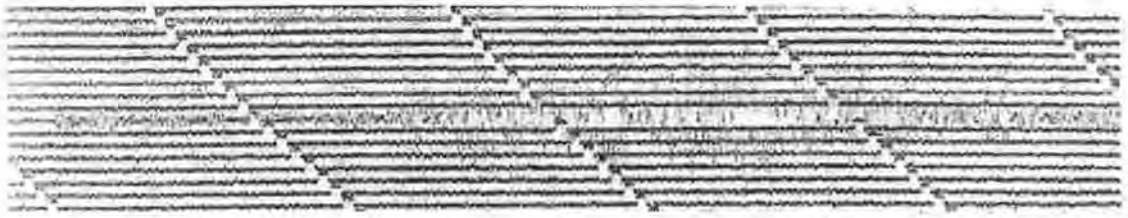

Fig 6: Adelaide short-period seismograms of the 1972 Temora earthquake; E-W component at the top, N-S component in the middle, and vertical component at the bottom of the picture

The Warramunga records had very small amplitudes due to its epicentral distance of some 1,600km.

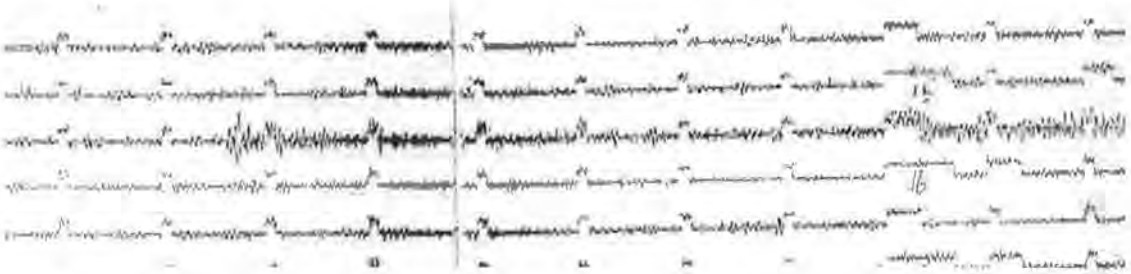

Fig 7: Warramunga short-period seismogram of the 1972 Temora quake (Z-component)

3. ANALYSIS

These seismograms are what we could retrieve from the regional stations in Australia to analyse the Temora earthquake which occurred in 1972. Most of the records are difficult to read precisely both in terms of phases and amplitudes and the results presented here are our best effort with the available material.

Based on our readings of the seismograms and using EQLOCL program with constrained depth of 10 km and magnitude formula for Southeast Australia, we produced the following table:

Station name	P-arrival		S-P time (s)	ML
	Observed	Residual		
CAN	15:23:04.9	-0.12	20	>3.5
RIV	15:23:24.6	+0.08	25	4.4
TOO	15:23:32.5	+0.13	46	4.4
ADE	15:24:19.6	-0.09	73.4	4.4

Table 1: Seismogram readings for the Temora earthquake

All S readings were difficult to confirm accurately, but in this analysis we had better definition of the S-phase at least on one station - Toolangi. The magnitude deducted

from the CAN station is just indicative, because the short-period records were clipped. Our origin time ($15^h22^m35.97^s$) and epicentre calculation (34.128±0.062°S and 147.344±0.053°E) was within the errors of the previously published solution for which we could not find the original readings: ISC - $15^h22^m35.8^s$, 34.21±0.19°S and 147.33±0.30°E, shallow depth 33 km, and Denham *et al.* in 1985 - $15^h22^m36^s$, 34.22°S and 147.47°E, shallow depth respectively.

The newly calculated magnitude value of 4.4 is consistent at all of the stations. These results show that calculation using several observations can produce more stable solution than cases when only one station is used. We plan to apply this approach in future to review the important earthquakes in the database and reduce the uncertainty in their magnitude and epicentral location.

4. SUMMARY AND DISCUSSION

The Earthquake Hazard and Neotectonics group (EHN) at GA have re-evaluated the 1972 Temora earthquake which occurred on 25th of February, in order to improve the seismic hazard estimates in Southeast Australia. That is important for the definition of zones and determination of magnitude-frequency relationship, in the process of creating input parameters for the hazard calculation in general.

Previously that earthquake appeared as a moderate size earthquake with magnitude estimates varying according to different authors between 4.0 and 5.1 on the Richter scale. We collected available Australian seismograms of the event and analysed them in detail. We used EQLOCL program for magnitude and location calculation to compare our solution with the information which appeared in the Bulletin of the International Seismological Centre (ISC Bulletin, 1972). The records are difficult to read precisely both in terms of phases and amplitudes and the results presented here are our best effort with the available material.

We also searched the newspapers for reports of the earthquake, and other relevant information at that time which might have helped to form an isoseismal map of the event. No explicit references were found and no isoseismal map was compiled.

On the basis of our readings of the seismograms and using EQLOCL program for calculation of earthquake magnitude and location, we revised the local magnitude of the Temora 1972 event to 4.4. Our epicentral location remained between the errors of the published solutions which indicates that no significant adjustments are needed for the current velocity model of the Sydney basin. These findings might have implications to the relationship which describes the occurrence of earthquakes with magnitude 5+ in the Southeastern Australia, in a way that it diminishes the perception of the seismic potential in that zone and consequently lowers the hazard.

Over the next few years GA plans to validate and recalculate the largest events in the Australian earthquake catalogue using modern location software, velocity models and magnitude formulas.

ACKNOWLEDGEMENTS

The author is thankful to Mark Leonard and Angela Bullock from GA for their help in seismic analysis and reviewing the material and Kevin McCue from the ASC for his co-operation during the searching of the archives and his scientific guidance.

REFERENCES

Bulletin of the International Seismological Centre, February 1972. Edinburgh, UK.

Denham, D., Jones, T., and Weekes, J. (1985) The 1982 Wyalong earthquakes (NSW) and recent crustal deformation. BMR Journal of Australian Geology and Geophysics. No. 9, pp. 255-260.

Drake, L. (1974) The seismicity in New South Wales. Journal and Proceedings of the Royal Society of New South Wales. Vol. 107, pp. 35-40.

EXPERIMENTAL INVESTIGATION INTO VIBRATION CHARACTERISTICS OF A CRACKED RC T-BEAM

WIRTU L. BAYISSA[1*] AND N. HARITOS[2]
UNIVERSITY OF MELBOURNE

AUTHORS:

[1]Mr. Bayissa is a PhD student in Civil Engineering at the University of Melbourne. He completed B.Sc. in Civil Engineering from Addis Ababa University (Ethiopia) and M.Tech from Aligarh Muslim University (India). He has 3 years of experience in the construction field and teaching. His research interests include: FEA of plates and shells; structural damage identification and structural dynamics.

[2]Assoc. Professor Nicholas Haritos is a Reader in Civil Engineering at The University of Melbourne. He has over 32 years of post-graduate experience in research, academia and specialist consulting. His research interests include: structural dynamics of both land-based and offshore structures; hydrodynamics; condition/capacity assessment of bridge structures; experimental modal analysis testing and computers in modelling, simulation and control.

ABSTRACT:

The presence of damage causes changes in the physical properties of a structure which in turn alter its dynamic response characteristics. The monitoring of the changes in the response parameters of a structure has been widely used for the assessment of structural integrity. However, it has proven to be challenging to identify and estimate damage severity when this damage is induced by cracks. Irregular variations in the measured vibration response characteristics have been observed depending upon whether the crack is *closed*, *open* or *breathing* during vibration, the degree of severity and modal type. These variables consequently affect the effectiveness of structural integrity assessment. The main focus of this paper is to investigate the dynamic characteristic behaviour of a RC T-beam element subjected to four different crack states and attempt to identify optimal parameters common to all types of crack condition which can be used for structural condition assessment.

1. INTRODUCTION

The analysis of the dynamic response characteristics of a structure subjected to excitation and the subsequent monitoring of the changes in the response parameters is an effective tool for the assessment of structural integrity. These response parameters characterise the 'global' properties of the structure and have been widely used for in-service monitoring and evaluation of structural integrity after extreme events such as earthquakes. However, problems have been identified when these parameters are used for damage identification studies in RC T-beam subjected to flexural cracking. The irregular variations observed in the response parameters during the damage identification studies affected the capability to correctly identify damage. Three primary sources were anticipated for these variations: local stiffness discontinuity due to '*breathing*' of cracks; a geometric influence caused by lack of proper constraints at the end supports and amplitude nonlinearity due to impulsive events at the crack interface.

In the past, various researchers conducted investigations into the vibration characteristics of defective structures (Dimarogonas, 1996; Brandon et al., 1999). The spectral contents, phase history and other similar properties have been used for the identification of nonlinear response behaviour in a defective cantilever beam (Brandon, 1998; Brandon and Sudraud, 1998; Léonard et al., 2001). Considerable effort has also been placed on analytical modelling for the prediction of the vibration properties in structural elements subjected to '*breathing*' cracks (Chu and Shen, 1992). However, many of these studies are based on controlled experiments conducted on simple structural elements, specific material type and crack conditions. Therefore, it is difficult to extend these techniques to structural integrity assessment of complex situations such as RC structures subjected to arbitrary and multiple cracks. The objective of this paper is, therefore, to conduct an investigation into the response characteristic behaviour of a simply supported RC T-beam element subjected to multiple and arbitrary crack states. The response parameters obtained from the following crack conditions were used in conjunction with a simple analytical bilinear model for conducting this study:

LC0: initial 'pristine' condition where the beam is subject to minor cracks due to self weight; represents the *closed crack state;*
LC1: intermediate flexural cracking condition where the beam is subjected to an added mass equivalent of 1.0 kPa; represents the progressively growing *open crack state;*
LC2: increased flexural cracking condition induced by an added mass equivalent of 2.25kPa; represents the progressively growing *fully open crack state;*
LC3: *breathing crack state* due to opening and closing of cracks during vibrations, after removal of ***LC2*** loading condition.

2. SIMPLE ANALYTICAL MODEL FOR DIFFERENT CRACK CONDITIONS

The simulation of a *breathing* crack state in a Single Degree of Freedom (SDOF) system was presented using a piecewise linear time record based on a bilinear stiffness model concept. The spectral contents for the simulated free vibration response of the undamped SDOF system were determined using 2048 data points obtained from 20 cycle time records for each crack condition (Fig. 1a). The overlaid plots of the response spectra for different crack states indicate that the spectral pattern for the *breathing* crack

is very different from others. Higher frequency harmonics were observed at integer multiples of the fundamental frequency of the bilinear model (Fig. 1c). The phase plane also indicates the existence of two foci and some abrupt changes in velocity of the bilinear model which are indicative of impulsive events at the crack faces. These observations will be used in the following sections for investigation of similar behaviour in the experimental results.

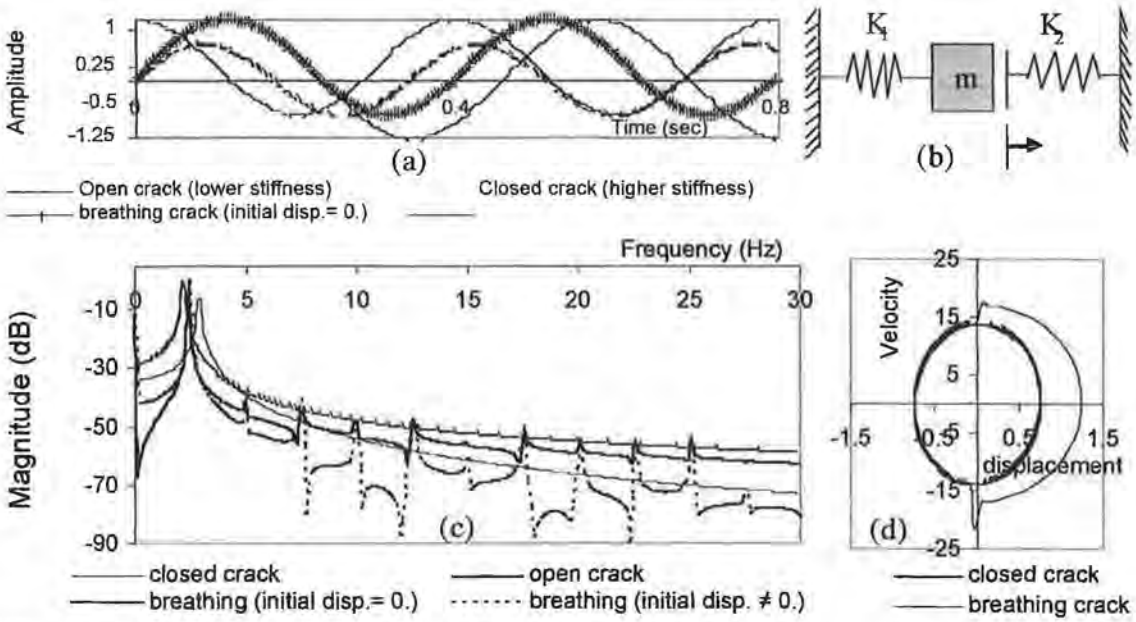

Figure 1 Free vibration response analysis for undamped SDOF system: (a) piece-wise linear time record; (b) bilinear stiffness model; (c) response spectra; (d) phase plane

3. EXPERIMENTAL STUDIES

The 9.4m long simply supported RC T-beam was constructed at the University of Melbourne using normal strength concrete for the flat slab section $(1.7m \times 0.12m)$ and high strength concrete for the web section $(0.25m \times 0.25m)$, (Haritos, 2003). A series of dynamic tests were conducted involving the measurement of vibration responses for different crack conditions using accelerometers while an impact hammer was used for the source of excitation. Consequently, FFT and modal analysis were performed on the response data to obtain Frequency Response Functions (FRFs) and modal parameters in the frequency domain. The relevant analysis results are presented, (see Figs. 2-5).

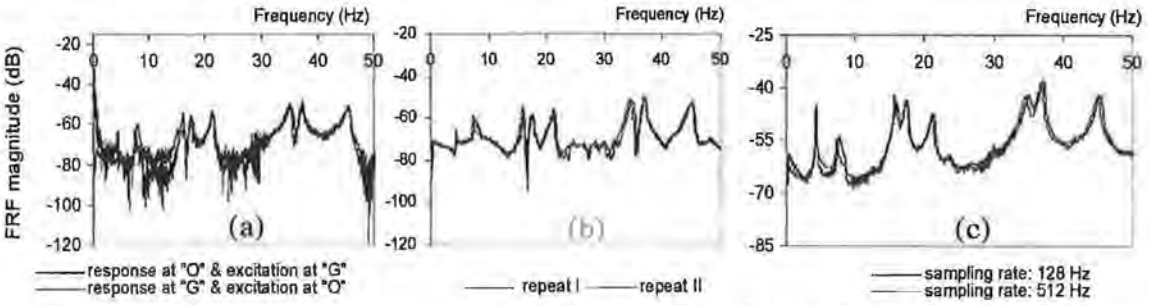

Figure 2 FRF data quality assessment: (a) reciprocity check; (b) amplitude linearity check; (c) measurement repeatability check (for *breathing* crack condition: ***LC3***)

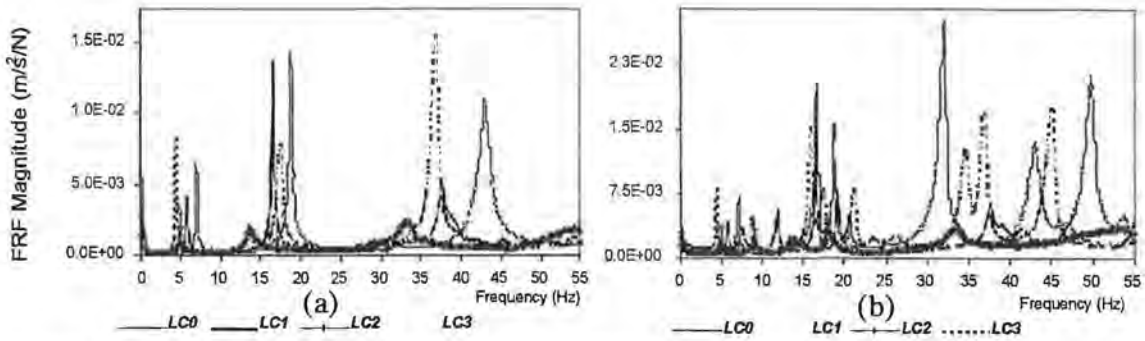

Figure 3 Comparison of ensemble average FRFs for all crack conditions (a) bending dominated modes; (b) all modes

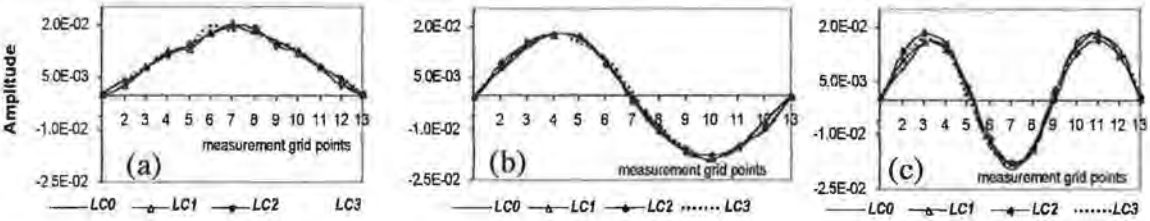

Figure 4 Comparison of mass-corrected mode shapes for flexural modes and for different crack conditions: (a) first mode; (b) second mode; (c) third mode

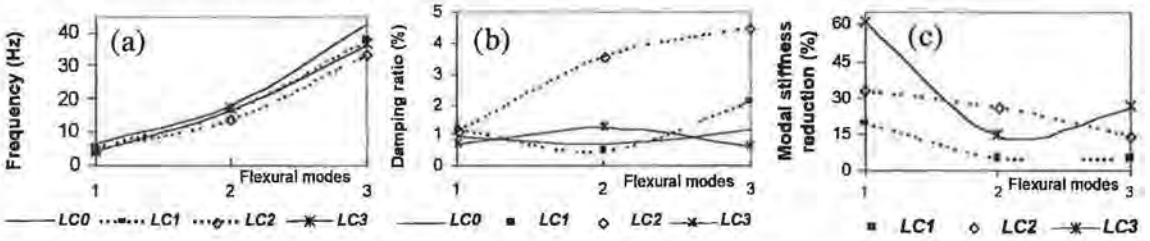

Figure 5 Comparison of modal parameters and modal stiffness properties for flexural modes: (a) natural frequencies; (b) modal damping ratios; (c) modal stiffness reduction

5. DISCUSSION ON VARIATIONS IN THE RESPONSE PARAMETERS

(i) Natural frequency: The general consensus in the literature is that the natural frequencies for the closed crack state should be higher than those from other crack states and the frequencies for the breathing crack state should lie between those for the closed and open crack states. However, the current analysis results indicate substantial inconsistent variation across the modes, especially for non-flexural modes (Fig. 3 and 5a). For the first mode, the frequency for the breathing crack condition is lower than those from all other crack conditions. For other modes, the frequencies from the ***LC2*** exhibited the lowest value while the breathing crack frequencies tend to straddle between those from ***LCO*** and ***LC1***. However, the changes in the frequencies for the ***LC1*** and ***LC2*** cases are influenced by the combined effects of the changes in the stiffness *and* mass properties. This fact can be observed clearly from the relationships between undamaged and damaged parameters obtained from the Eigen equation in terms of its key parameters such as mode shapes for the closed crack condition (ϕ); changes in the frequencies $(\Delta\omega)$; changes in mode shapes $(\Delta\phi)$; changes in stiffness and mass matrices (ΔK), (ΔM), respectively, and given by:

$$\Delta\omega^2 = \frac{\{\phi\}^T[\Delta K]\{\phi\} - \omega^2\left(\{\phi\}^T[\Delta M]\{\phi\} + \{\phi\}^T[\Delta M]\{\Delta\phi\}\right)}{\{\phi\}^T[\Delta M]\{\phi\} + \{1\}} \quad (1)$$

(ii) Modal stiffness: The change in modal stiffness for flexural modes, as determined using equation (1), indicates regular variation across the modes except for the second mode (Fig. 5c). The maximum percentage reduction relative to the undamaged state (***LC0***) was observed for the *breathing* crack condition (***LC3***) and for the first mode.

(iii) FRF amplitudes: Damage reduces local stiffness and increases flexibility of a structural element. Therefore, the peak FRF amplitudes for ***LC0*** are expected to be lower while those from ***LC3*** are higher than those from other states. However, the present experimental results reveal the difficulties associated with conducting any practical comparison for peak FRF amplitudes for different crack conditions, especially for non-flexural modes (Fig. 3b). For flexural modes, more regular behaviour was observed for ***LC0*** and ***LC3***. On the other hand, the FRF amplitudes from the fully open crack state were found to be the lowest for all modes and crack conditions. One of the possible explanations for this irregular variation is the influence of the added mass on the FRF amplitudes. The following equation derived from the Eigen equation indicates the influence of combined changes in stiffness and mass properties on the amplitude of inertance FRFs:

$$\overline{H}(\omega) = \frac{-\omega^2}{[\overline{K}] - \omega^2[\overline{M}]} = \frac{-\omega^2 H(\omega)}{H(\omega)\left([\Delta K] - \omega^2[\Delta M]\right) - \omega^2} \quad (2)$$

where $\overline{H}(\omega)$ is the inertance FRF for the damaged states, $H(\omega)$ is the inertance FRF for the undamaged state, $[\overline{K}] = [K] + [\Delta K]$ and $[\overline{M}] = [M] + [\Delta M]$.

Another possible explanation for the irregular variation is that the changing nature of the crack condition during experimental tests due to the influence of the added mass causes time-dependent variation in the response data resulting in a so-called non-stationary response. It is also reported in the literature that in the case of an open crack state, the capability of the crack zone to transmit vibration tends to degrade since the vibration sensor could be measuring the responses from that part of the uncracked beam which is stiffer than the entire beam.

(iv) Mode shapes: Similar to other modal parameters, the changes in mode shape increase with an increase in damage severity. In the current results, the variations observed in mode shapes were induced by the combined effects of the changes in stiffness and mass properties. The overlaid plots for mass-corrected mode shapes for different crack states are presented for flexural modes (Fig. 5). Though these changes are consistent across the modes and across crack states, they were not sensitive enough to clearly identify stiffness changes in the T-beam due to arbitrary and multiple cracks.

(v) Modal damping: Modal damping increases with an increase in crack severity, amplitude of vibration and loading intensity. Though the current results exhibit this tendency for some crack conditions in the flexural modes, damping values are

inconsistent particularly for the breathing crack state. Moreover, the damping values reached their maximum for the partially opening crack condition (***LC2***), (Fig. 5b).

5. CONCLUSIONS

This investigation has provided useful information regarding response parameters obtained from progressively induced crack conditions in a RC T-beam element. However, our goal for identification of consistent response parameters which can be used reliably for structural integrity assessment was hampered by encountering substantial irregularities in the response parameters across the modes and across crack condition states. The following conclusions can be drawn from this study:

- The dynamic testing of a structure with high level mass loading may not be reliable since it may cause non-stationary behaviour in the response signals.
- The nature of the harmonic characteristics and the absence of higher mode participation observed in the fully open crack case is a strong indication of the existence of geometric nonlinearity. Furthermore, the observation of high correlation in the non-flexural modes in all crack states indicate that the end supports of the test beam provided improper (non-linear) torsional restraint.
- There is no evidence for the occurrence of *breathing crack* condition and impulsive events of cracks since there is no similarity between spectral patterns observed from analytical and experimental results. Moreover, reciprocity and linearity checks conducted on the FRF data indicate no evidence of amplitude nonlinearity.

Finally, the modal stiffness reduction appears to be more sensitive to crack states, as expected, but for the test T-beam investigated here the reduction did not appear consistent between modes. Consequently, use of response parameters in combination would be more reliable than using them individually for structural integrity assessment, as each such response parameter is not without some form of deficiency.

REFERENCES

Brandon, J. A. (1998) Some insights into the dynamics of defective structures, Proceedings of the Institution of Mechanical Engineers Part C- Journal of Mechanical Engineering Science, 212, 441-454.

Brandon, J. A., Stephens, A. E., Lopes, E. M. O. and Kwan, A. S. K. (1999) Spectral indicators in structural damage identification: a case study, *Proceedings of the Institution of Mechanical Engineers Part C- Journal of Mechanical Engineering Science*, Vol 213, pp 411-415.

Brandon, J. A. and Sudraud, C. (1998) An experimental investigation into the topological stability of a cracked cantilever beaM, *Journal of Sound and Vibration*, Vol 211, pp 555-569.

Chu, Y. C. and Shen, M.-H. H. (1992) Analysis of forced bilinear oscillators and the application to cracked beam dynamics, *AIAA Journal*, 30, pp 2512-2519.

Dimarogonas, A. D. (1996) Vibration of cracked structures: A state of the art review, *Engineering Fracture Mechanics*, Vol 55, pp 831-857.

Haritos, N. (2003) Static and dynamic testing of two floor beams, Melbourne University Private Ltd Report, MUP 2002-151 (2).

Leonard, F., Lanteigne, J., Lalonde, S. and Turcotte, Y. (2001) Free-vibration behaviour of a cracked cantilever beam and crack detection, *Mechanical Systems and Signal Processing*, Vol 15, pp 529-548.

RESPONSE SPECTRUM CHARACTERISTICS OF RECORDED STRONG GROUND MOTIONS IN SWWA

HONG HAO[1], BRIAN GAULL[2]
[1]SCHOOL OF CIVIL AND RESOURCE ENGINEERING, THE UNIVERSITY OF WESTERN AUSTRALIA
35 STIRLING HIGHWAY, CRAWLEY, WA 6009, AUSTRALIA
[2]GURIA CONSULTING, P.O. BOX A122, AUSTRALIND, WESTERN AUSTRALIA

AUTHORS:

Hong Hao is a professor of structural dynamics in the School of Civil and Resource Engineering, the University of Western Australia. He received his PhD degree in Department of Civil Engineering, University of California at Berkeley. Before joining UWA in 2002, he worked as a post-doc researcher in Seismographic Station in UC Berkeley and was an associate professor in Nanyang Technological University in Singapore. His research interests are structural dynamics, earthquake and blast engineering.

Brian A Gaull is director of Guria Consulting. He has been interested in Seismic Hazard and Strong Ground Motion since his first appointment with GA (formerly BMR) over 30 years ago. Two decades of such experience enabled him to set up Guria Consulting in Western Australia more then 13 years ago.

ABSTRACT

This paper studies the characteristics of spectral accelerations of ground motions in Southwest Western Australia (SWWA). The available strong ground motion records on rock and soil sites in SWWA are normalized to 1.0g and their acceleration response spectra are respectively estimated and compared with the corresponding design spectra in the current Australian seismic code. Ground motion time histories on rock site for SWWA conditions are also stochastically simulated according to a modified eastern North America (ENA) model. The acceleration response spectra of the simulated motions are also calculated and compared with the design spectrum and the spectra of the recorded motions. Discussions on the suitability of the code spectra are made.

Response Spectrum Characteristics of Recorded Strong Ground Motions in SWWA

Hong Hao[1], Brian Gaull[2]

[1]School of Civil and Resource Engineering, the University of Western Australia

35 Stirling Highway, Crawley, WA 6009, Australia

[2]Guria Consulting, P.O. Box A122, Australind, Western Australia

ABSTRACT

This paper studies the characteristics of spectral accelerations of ground motions in Southwest Western Australia (SWWA). The available strong ground motion records on rock and soil sites in SWWA are normalized to 1.0g and their acceleration response spectra are respectively estimated and compared with the corresponding design spectra in the current Australian seismic code. Ground motion time histories on rock site for SWWA conditions are also stochastically simulated according to a modified eastern North America (ENA) model. The acceleration response spectra of the simulated motions are also calculated and compared with the design spectrum and the spectra of the recorded motions. Discussions on the suitability of the code spectra are made.

1. INTRODUCTION

Owing to lack of strong ground motion records, the design response spectra in the current Australian Standards for Earthquake Loads [Standards Australia 1993] were developed based on recorded motions elsewhere around the world, and mainly from interplate regions [Somerville, et al. 1998]. High stress drops from events in intraplate regions of the world result in higher frequency contents of ground motions than corresponding events in interplate regions. This will affect the ground motion attenuation as well as the response spectrum shape. Therefore the reliability of the design response spectrum in the Australian Standards for earthquake loads needs be examined.

A previous study analysed the response spectra of ground motions from 6 intraplate earthquakes and recommended response spectra for Australia [Somerville, et al. 1998]. In that study unfortunately none of the 6 earthquakes analysed occurred in Australia. Other authors used earthquake ground motion attenuation model for intraplate events in eastern North America (ENA) [Lam, et al. 2000] together with the local geological parameters in predicting the ground motion response spectra for Australian earthquakes. A recent study that compares the ENA seismic models with the recorded strong ground motions in southwest Western Australia (SWWA) indicated significant discrepancies between the ENA models and the recorded motions in SWWA [Hao and Gaull 2004a], and a modified ENA model for predicting ground motions in SWWA was subsequently proposed [Hao and Gaull 2004b].

In this study, the normalized response spectra of the available recorded motions in SWWA will be calculated and compared with the design response spectrum in the Australian Code [Standards Australia 1993]. Because only 14 triaxial ground motion time histories from 7 earthquake events of magnitude ranging from ML4.1 to ML6.2 and epicentral distance from 6 km to 196 km are available, ground motion time histories are also simulated in the study according to the modified ENA seismic motion model [Hao

and Gaull 2004b]. In order to cover possible earthquake ground motion scenarios in SWWA, ground motions are simulated for earthquakes of magnitudes ranging from ML5.0 to ML7.5 and epicentral distances from 30 km to 200 km. The normalised response spectra of the recorded and simulated ground motions are calculated and compared with the design spectrum. Discussions on the reliability of the design response spectrum in current Australian Standards [Standards Australia 1993] are made.

Table 1 Lists of 14 recorded ground motions in SWWA

No	M_L	Epicenter	Dist (km)	Site	Depth (km)	PGA (mm/s²)			PGV (mm/s)		
						EW	NS	VE	EW	NS	VE
1	6.2	Cadoux	87	Granite	6	150	128	93	6.63	4.13	6.81
2	6.2	Cadoux	93	Granite	6	293	306	245	19.34	21.08	27.18
3	6.2	Cadoux	96	Thin alluvium/granite	6	220	170	149	26.90	12.21	10.03
4	4.5	Cadoux	6	Weathered Bedrock	5	2612	2888	921	27.63	27.81	15.69
5	4.5	Cadoux	8	Granite	5	1543	1008	939	26.14	11.39	9.28
6	4.5	Cadoux	13	Weathered Bedrock	5	439	474	558	9.73	8.85	10.54
7	5.5	Meckering	78	Granite	6	99	26	31	1.38	0.54	0.59
8	4.5	Cadoux	70	Rock	2	72	49	39	0.73	0.42	0.42
9	4.1	Meckering	25	Rock	6	139	116	48	1.20	0.65	0.29
10	4.1	Meckering	90	Weathered Bedrock	6	6	13	8	0.16	0.29	0.11
11	4.1	Meckering	120	Clay/alluvium	6	9	11	4	0.470	0.535	0.16
12	5.1	Burakin	193	Sand/mud/sand	2	6	4	3	0.19	0.19	0.10
13	5.2	Burakin	192	Sand/mud/sand	1	13	12	8	0.51	0.49	0.22
14	5.2	Burakin	196	Sand/clay	1	6	6	5	0.21	0.29	0.23

2. RECORDED GROUND MOTIONS IN SWWA

Table 1 lists the recorded ground motions used in this study, in which epicentral distance and depth are in kilometers. As indicated, records 1 to 10 are essentially from rock sites and 11 to 14 are on soil sites. The epicentral distances of the rock site motions range from 6 km to 96 km and those of the soil sites 120 km to 196 km. Peak ground acceleration (PGA) and velocity (PGV) of the corresponding records are also given in the table. Figures 1 shows typical recorded accelerations time histories.

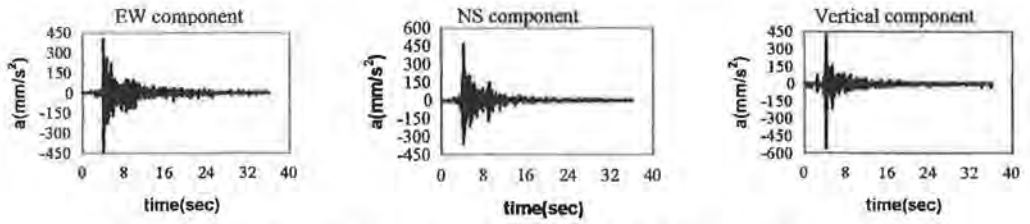

Fig. 1. Recorded ground acceleration time histories (record 6 in Table 1)

3. SIMULATED GROUND MOTIONS

A modified ENA seismic ground motion model was proposed to predict motions in SWWA. Using the geophysical parameters for Western Australia conditions, it was demonstrated that the modified seismic ground motion model could give reasonable prediction of the recorded motions in SWWA [Hao and Gaull 2004b].

Both earthquake magnitude and distance affect ground motion response spectral shape. Usually, ground motion from a larger earthquake has a wider response spectrum than a smaller event at the same distance, and the frequency contents of ground motions from an earthquake decreases with the distance. As supplements to the recorded motion, ground motion time histories on rock site in SWWA are simulated based on the modified seismic ground motion model. Table 2 lists the simulated events and the corresponding average PGA and PGV value from four simulations for each case.

Table 2 Lists of the simulated ground motions

ML	5.0				6.0					7.0						
D(km)	30	50	80	100	30	50	80	100	120	30	50	80	100	120	150	200
PGA	161	100	85	73	512	310	257	205	163	1391	793	660	561	455	339	217
PGV	1.54	1.11	1.02	0.97	5.72	3.54	3.13	2.85	2.62	12.5	11.2	10.0	9.76	9.26	8.50	7.29
ML	5.5				6.5					7.5						
PGA	288	178	121	103	861	479	377	325	259	2757	1840	1598	1384	1138	858	671
PGV	3.01	2.01	1.47	1.41	7.02	4.91	4.81	4.85	4.34	26.9	22.6	21.6	21.2	20.8	18.6	18.1

Figure 2 shows the simulated horizontal ground motion time history corresponding to ML7.5 and focal distance d=100 km. The simulation is carried out with the assumption that the ground motion time history is a modulated stationary random process. Each simulated time history is compatible with the ground motion spectrum model for SWWA. Only horizontal component of the ground motion is presented in this paper.

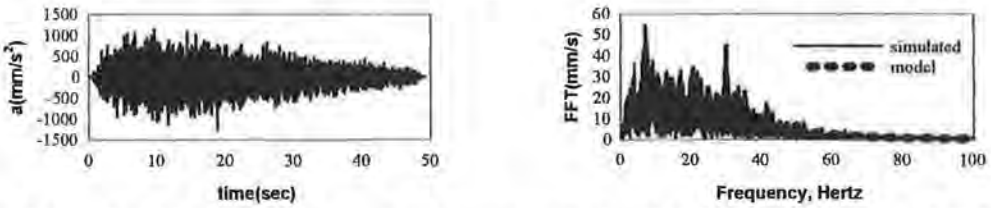

Fig. 2 Simulated horizontal ground motion on rock site (ML7.5, focal distance 100 km)

4. ACCELERATION RESPONSE SPECTRA

All the recorded motions are normalised to PGA=1.0g and their acceleration response spectra are calculated. Figure 3 shows the acceleration response spectra of the recorded motions on rock sites and the code design spectra with site factor S=0.67 and 1.0 for hard and soft rock. As shown, the code spectra in general overestimate the spectral accelerations of the recorded motions in the period range between 0.3 sec and 3.0 sec. This period range covers the fundamental vibration periods of most common structures. The code spectra underestimate spectral accelerations in the period range of 0.02 sec to 0.2 sec when compared with some of the recordings, implying they may underestimate seismic forces of very stiff structures.

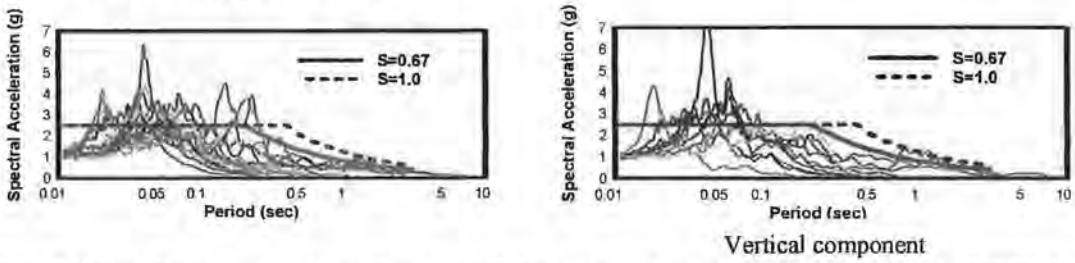

Vertical component

Fig. 3 Normalised spectral acceleration of the recorded motions on rock sites in SWWA

Figure 4 shows the mean, mean plus and mean minus one standard deviation of spectral accelerations of the recorded motions on rock sites. It shows that code spectrum overestimates mean normalised spectral acceleration for most periods, especially those of engineering significance with T≥0.1 sec.

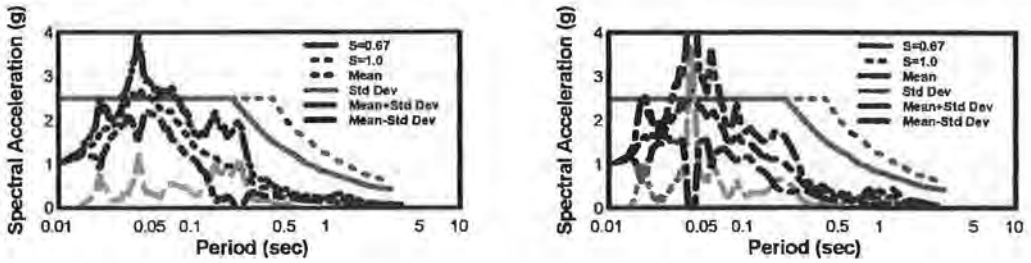

Fig. 4 Mean, standard deviation, mean plus and mean minus standard deviation of spectral accelerations of the recorded motions on rock sites in SWWA

The normalised spectral accelerations of the recorded motions on soil sites are shown in Figure 5. Similar to those on rock sites, the code spectra in general overestimate the spectral acceleration values, but might underestimate the spectral values in the period range of 0.1 sec to 0.5 sec. However, this period range may increase when data from larger magnitude events are available.

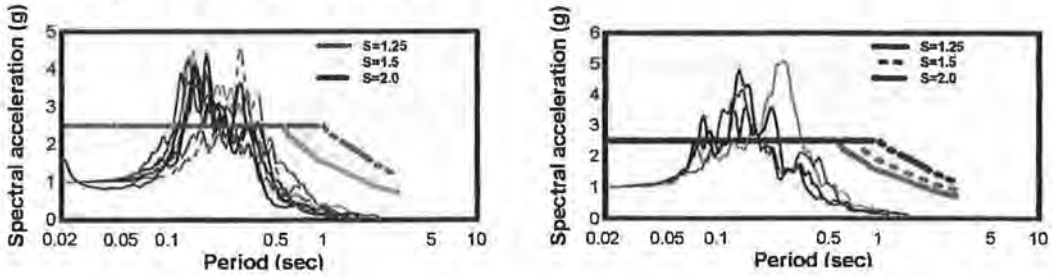

Fig. 5 Normalised spectral acceleration of the recorded motions on soil sites in SWWA

Figure 6 shows the normalised spectral accelerations of the simulated ground motions. Their mean values, standard deviation, mean plus one standard deviation and mean minus one standard deviation, as well as the code design spectra for rock sites are also shown in the figure. Similar observations made above can also be drawn here.

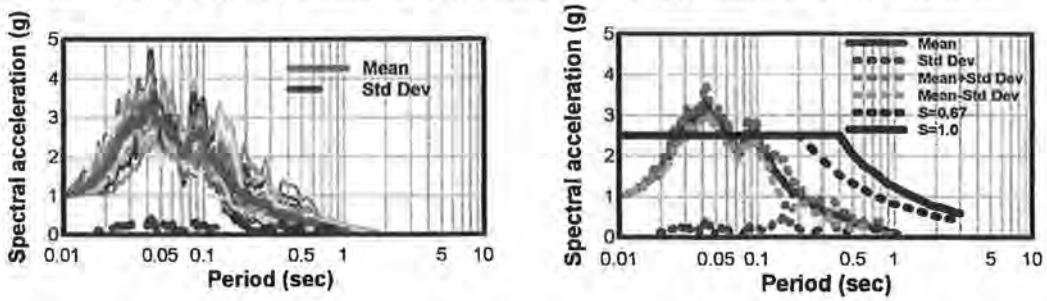

Fig. 6 Normalised spectral acceleration of the simulated ground motion

Figure 7 shows the comparison of the mean and standard deviation of the spectral accelerations of the recorded and simulated horizontal motions on rock sites. The mean

spectral acceleration of all the motions (recorded and simulated) and the code design spectra are also shown in the figure. As shown, the mean spectral acceleration of the simulated motions is very similar to that of the recorded motions, but is slightly wider and has slightly larger spectral acceleration values. This is because the number of records used in the analysis is very limited and biased towards the lower earthquake magnitudes. The code design spectra in general overestimate the spectral acceleration values except in the period range of 0.03 sec to 0.06 sec.

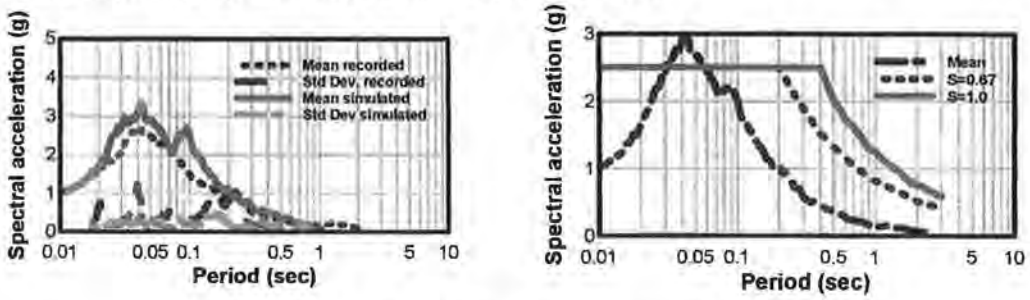

Fig. 7 Comparison of the mean spectral accelerations

5. CONCLUSIONS

Normalised spectral accelerations of the recorded and simulated ground motions in SWWA are calculated and compared with the code design spectra. It is found that the design spectra specified in the current seismic code in general overestimate the spectral acceleration values, but they might underestimate spectral accelerations of ground motions on rock sites in the period range between 0.03 sec and 0.06 sec, and between 0.1 sec and 0.5 sec for ground motions on soil sites. More studies of the SWWA strong ground motion characteristics are necessary, especially for motions on soil sites.

REFERENCES

Hao, H. and Gaull, B. (2004a) Comparison of intraplate ENA seismic model and recorded strong motion in Western Australia, Accepted, The Eighth International Symposium on Structural Engineering for Young Experts, August, 2004, Xi'an, China

Hao, H. and Gaull, B. (2004b) Prediction of Seismic Ground Motion in Perth Western Australia for Engineering Application, Paper No. 1892, Proceedings of the 13Th World Conference on Earthquake Engineering, August 2004, Vancouver, Canada.

Lam, N, Wilson, J., Chandler, A. and Hutchinson, G. (2000) Response spectrum modelling for rock sites in low and moderate seismicity regions combining velocity, displacement and acceleration predictions, Journal of Earthquake Engineering and Structural Dynamics, Vol. 29, pp1491-1525.

Somerville, M., McCue, K. and Sinadinovski, C. (1998) Response spectra recommended for Australia, Proceedings of Australasian Structural Engineering Conference, Auckland, October 1998, pp439-444.

Standards Australia (1993)Australian Standard: Minimum design loads on structures, Part 4: Earthquake loads – AS1170.4 – 1993',

ANCHORAGE OF CRITICAL ELEMENTS IN A MOMENT-RESISTING STEEL I BEAM-TO-CFT COLUMN CONNECTION

H. YAO[1], H. M. GOLDSWORTHY[2], E. F. GAD[3]
UNIVERSITY OF MELBOURNE

AUTHORS:

1. PhD candidate, Department of Civil and Environmental Engineering, The University of Melbourne, Victoria 3010, Australia. Ph: (+61) 3 8344 4709, Fax: (+61) 3 8344 4616, E-mail: hyao@civenv.unimelb.edu.au
2. Senior Lecturer, Department of Civil and Environmental Engineering, The University of Melbourne.
3. Senior Lecturer at Swinburne University of Technology and Senior Research Fellow at The University of Melbourne.

ABSTRACT:

The behaviour and performance of Concrete-Filled Steel Tube (CFT) composite sway frames for seismically induced loads, depends on the strength, stiffness and ductility of the connections, and of the members adjacent to the joint. An innovative moment-resisting steel I beam-to-CFT column connection utilising blind bolts and bolt extensions is being developed to suit loading conditions for regions of low to medium seismicity.

This paper focuses on numerical modelling of the steel bolt extension anchored inside the concrete-filled steel tube. The rotational stiffness of the overall connection and the strength hierarchy within the connection are influenced greatly by the stiffness and strength of the anchorage of the extensions. A series of nonlinear springs is utilised to model the force-slip behaviour of the extensions in an iterative solution algorithm. This approach is capable of predicting the pull out behaviour of an extension bar anchored in the confined concrete of the joint. The analytical model is compared with the experimental results from pull out tests of the straight bar and the cogged bar which simulate the bolt extensions.

Keywords: Bond and anchorage, slip, cog extension, confinement, analytical modelling, nonlinear spring.

1. Introduction

The Concrete-Filled Steel Tube (CFT) Structural System is a new system with excellent structural and architectural features. The behaviour and performance of CFT composite sway frames for seismically induced loads depends on the strength, stiffness and ductility of the connections, and of the members adjacent to the joint. However, one of the difficulties in using this type of construction is the problem of how to connect concrete-filled circular steel columns to composite beams without site welding. An innovative moment-resisting beam-to-circular column connection with blind bolts and extensions is being developed to achieve this goal with particular emphasis on loading conditions for regions of low to medium seismicity (Gardner and Goldsworthy 2004, Yao et al. 2003). This connection is intended to have sufficient stiffness to be regarded as a rigid connection, and sufficient strength such that plastic behaviour will be restricted to the adjoining members.

The details of the proposed connection are shown in Figure 1. The beam flanges are connected to the circular hollow section (CHS) column by a built-up T-section consisting of a curved endplate and a flared horizontal web-plate cut into a curved shape at the end to fit with the endplate. The T-sections are attached to the tube wall by blind bolts, and are anchored back into the concrete within the tube by extensions welded on to the bolt heads. The bolt extensions consist of Grade 500, Type N, reinforcing bars with a cog. In the design of the bolts and endplates, the simplifying assumption has been made that the beam flanges transmit all the bending moment, the compression force being resisted by bearing, and the tension force being resisted by the bolts and extensions, together with membrane action in the tube.

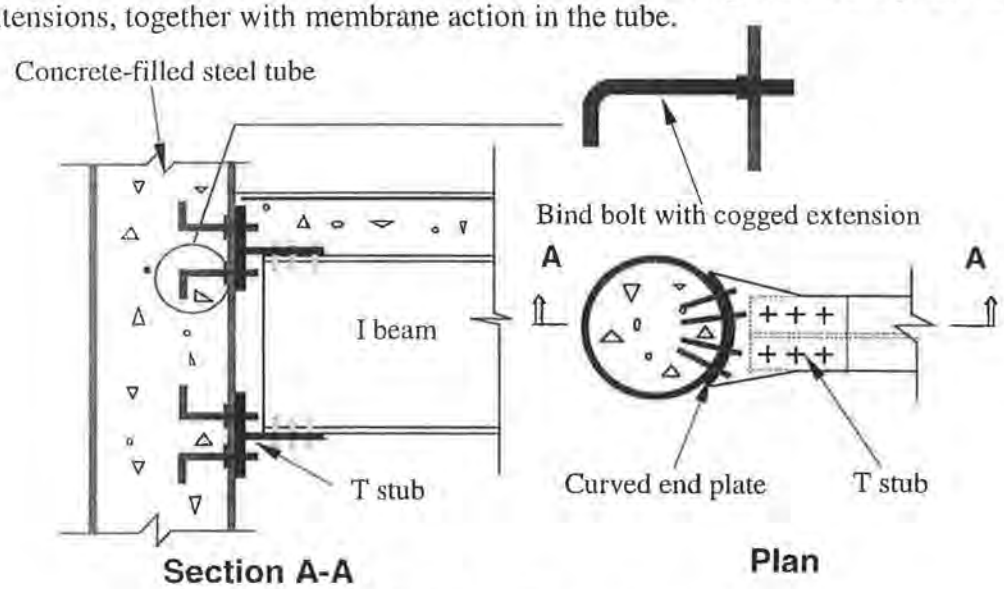

Figure 1: Beam-Column Connection

A series of preliminary tests have been performed on the critical T-section connections in tension and have given promising results (Gardner and Goldsworthy 2004). Understanding of the behaviour of each component of the connection is essential to the evaluation of the capacity, ductility and energy dissipation for the connection. Accurate modelling of the behaviour of these connections and matching it to the observed behaviour will lessen the need for further expensive experimental testing. Proper

modelling of a composite connection requires the accurate representation of all the key components. Developing analytical models which are capable of simulating the anchorage of the extensions in the concrete-filled circular steel tube is a critical part of overall modelling of the connection.

2. Modelling strategy of connection

The moment-resisting steel I beam-to-CFT column connection can be modelled by a series of individual spring elements, which represent the different force-deformation behaviour of the various components of the joint. The overall model is illustrated in Figure 2. The springs A and A' simulate the stiffness and capacity of the curved endplate of the T stub connecting the steel I beam and circular column. The springs B and B' simulate the stiffness and capacity of the anchorage of the extension within the confined concrete. In addition, springs C and C' simulate the membrane action of the tube filled with the concrete core. These spring elements form a structural hierarchy of force transfer mechanisms within the beam to column connection.

This paper focuses on the numerical modelling of the steel bar extension anchored in the concrete filled steel tube (spring B).

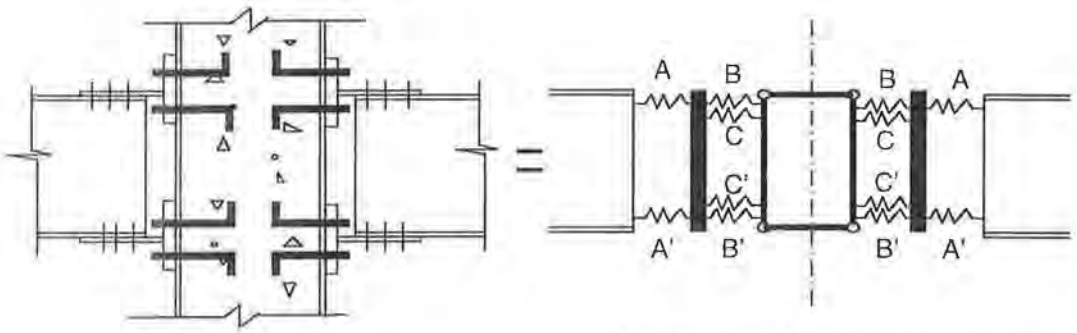

Physical connection Equivalent analytical representation

Figure 2: Overall Model of Beam-Column Connection

3. Analytical model of bar extension

3.1 Model assembly

3.1.1 Straight bar anchored in the concrete

The straight bar within the concrete can be divided into n segments with n+1 associated nodes. In each segment, there are two types of coupled elements. One type is a steel element, which simulates the stretching of the steel bar, and the other is a bond element, which simulates the interaction between the steel bar and the surrounding concrete. The discretization of the straight bar is illustrated in Figure 3.

3.1.2 Cogged bar anchored in the concrete

The cogged bar is regarded as two parts, straight portion and bent portion. The bent portion is idealized as a single nonlinear spring connecting the end of the straight bar to the concrete (Soroushian et al. 1988). The cogged model is idealized as Figure 4.

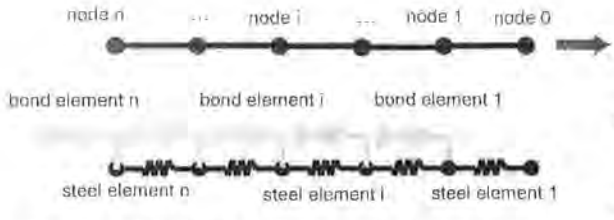

Figure 3: Model of straight bar in the concrete

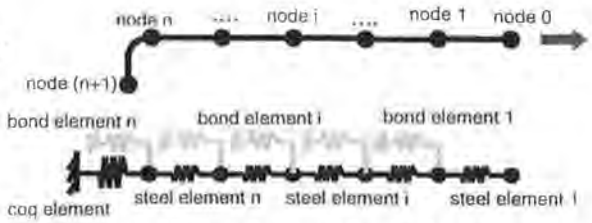

Figure 4: Model of cogged bar in the concrete

3.2 Nonlinear spring elements

3.2.1 Steel element

The behaviour of the steel element is based on a characterization of the force-deformation curve for each individual element segment. The force-deformation curve can be derived from a material model of the steel stress-strain relation. The monotonic envelope of the steel stress-strain relation is presented in Figure 5.

3.2.2 Bond Element

The bond stress between the concrete and the reinforcing bar within the straight length is related to the bar slip using the suggested relationship in the CEB-FIP model code (see Figure 6). This, in turn, is based on experimental work carried out at the University of California, Berkeley (Eligehausen et al. 1983).

3.2.3 Cog element

The behaviour of the cog element is based on an empirical hook pullout force-displacement relationship shown in Figure 7 (Soroushian et al.1988).

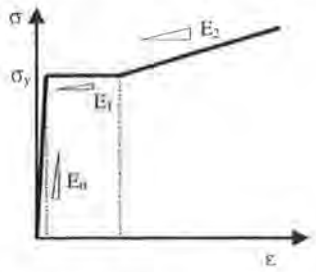

Figure 5: Steel stress-strain relationship

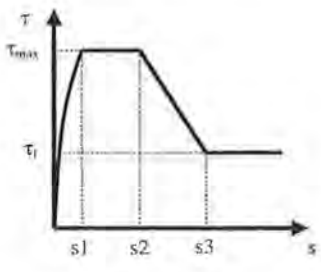

Figure 6: Bond stress-slip relationship

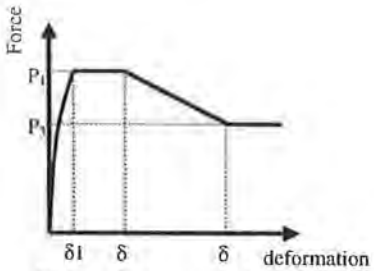

Figure 7: Force-deformation relationship for the cog

3.3 Nonlinear iteration algorithm

A solution algorithm has been developed and programmed. The algorithm is based on the element discretization presented earlier for the straight length combined with the

nonlinear spring properties. The loading on the extension bar is introduced by applying a known slip at the free end (node 0). The forces are calculated in the nonlinear springs. Then the displacements are deduced at the following node. This constructs an inner iterative loop for a typical segment process. The force in the last element and displacement for the last node are checked against the converged criteria. If the end value fails to pass, then the solution process is repeated again. An outer iterative loop is formed for the process.

3.4 Simulation of test done by Kankam

Double pull out tests on 25mm hot-rolled ribbed bars which had been fully instrumented internally were conducted to simulate the distribution of steel stress, bond stress, and slip between flexural cracks (Kankam 1997). The ribbed bar was embedded 200mm within an unconfined concrete prismatic block and was pulled from both ends. The variation of steel strain along the length of embedded bars was directly measured. Using symmetry, the bar is assumed to be anchored at the midpoint between the cracks and pulled from the end at the crack. This length of embedded bar is divided into 8 segments in the analytical model. Unconfined concrete and good bond conditions are applied to define the properties of nonlinear spring elements. Figures 8 and 9 compares results from the analytical model and experimental test for the distribution of steel stress and slip along the embedded ribbed bar.

The analytical modelling method was also benchmarked against the single sided pullout tests (Eligehausen et al. 1983) which represented the confined region of a concrete beam-column joint.

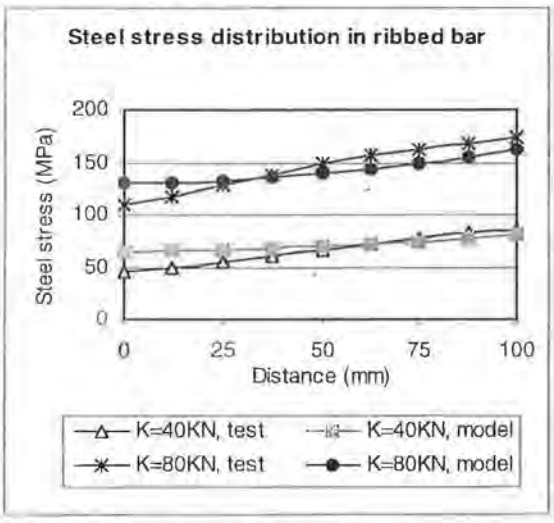

Figure 8: Steel stress distribution in ribbed bar

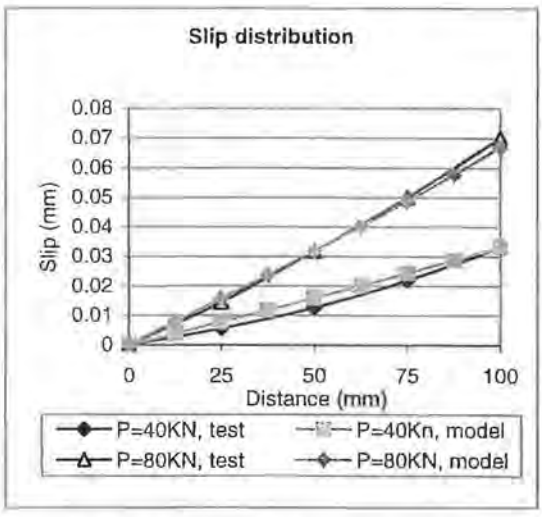

Figure 9: Slip distribution along ribbed bar

4. Experimental program at the University of Melbourne

4.1 Pull-out tests

Pull-out tests of the straight bar and cogged bar respectively, both embedded in concrete-filled circular steel tubes, were executed at the University of Melbourne. Table 1 lists the details of the specimens.

Parameter of straight bar and cogged bar	Parameter of tube:
Diameter of N type reinforcing bars:16mm Straight bar embedded length: $20d_b$=320mm Cogged bar bend radius: $4d_b$=64mm Cogged bar horizontal portion: $4.75d_b$=76mm Cogged bar vertical cog: $12d_b$(192mm)	Grade 350 circular steel tube Diameter (D) =323.9mm Thickness(t) =6.0mm D/t ratio =54.0 Infilled concrete: 50MPa at 28days

Table 1: specimen features

4.2 Loading and instrumentation

The bar is loaded in increments of roughly 15kN at 1 minute intervals by a hand-pump jack. The test is terminated when either the bar is pulled out of the steel tube or the bar fractures. In order to measure the total slip at the edge of the circular steel tube, a pin ring is gripped to the bar at the edge of the tube, and two LVDT set on the pin with their needles against the tube wall. Figures 10 and 11 demonstrate the setup of the pullout tests on the straight bar and cogged bar respectively. The load-slip curves in terms of the slip of the bar relative to the concrete have been plotted against the load on the bar.

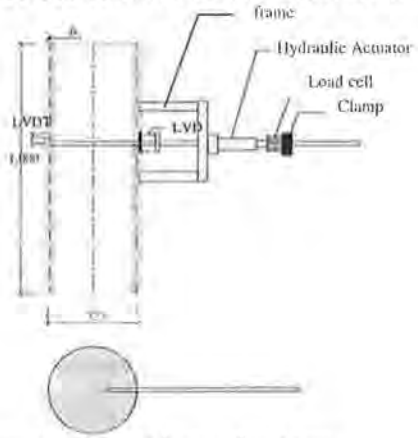

Figure 10: Straight bar pull out test

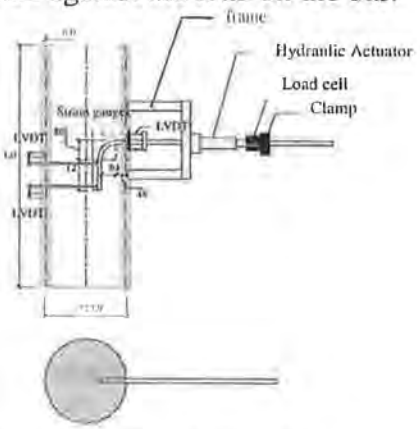

Figure 11: Cogged bar pull out test

5. Comparison of analytical model and test results

For the straight bar pullout test, the analytical model divides the bar of 320mm length into 16 segments associated with the coupled steel elements and bond elements. Confined concrete and normal bond conditions are applied to determine the element properties. The analytical result matches the test result well in terms of the load-slip relationship illustrated in Figure 12.

In the cogged bar pull out test, the cogged bar is composed of a 76mm long straight part and a standard cog stipulated in ACI 318-02. The straight portion is divided into 9 segments. The analytical model utilises a cog element attached to the end of the series of steel elements and bond elements. The discrepancy between the test and analytical model is small as displayed in Figure 13.

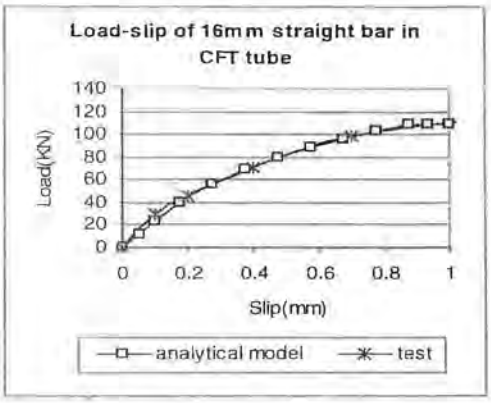

Figure 12: Load-slip of straight bar in CFT tube

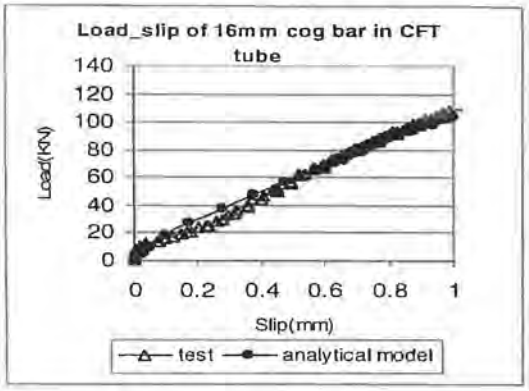

Figure 13: Load-slip of cog bar in CFT tube

6. Conclusion

An innovative moment-resisting steel I beam-to-CFT column connection utilising blind bolts and bolt extensions is being developed. The overall moment vs. rotation behaviour of the connection can be modelled by a series of individual spring elements, which represent the force-deformation relationship of the various components within the connection. The behaviour of one of the components, the bolt extensions anchored within the concrete-filled steel tube, has been investigated here. Previous testing of the T-stub connection in tension has shown that the effectiveness of the anchorage provided by the bolt extensions is essential in creating a connection with the desired stiffness and strength. Single bolt extensions have been considered in this study, although it should be noted that the behaviour of the anchored bolt group will be considered in future work.

The numerical model of the anchorage of the reinforcing bar extensions within either confined or unconfined concrete that has been developed here, is capable of predicting pull out behaviour of the straight bar and cogged bar as well as the steel stress, bond stress and slip distribution along the bar. Test data from previous tests by other researchers, as well as tests performed as part of this project has been compared with the model predictions. Excellent agreement has been achieved.

Acknowledgements

We greatly appreciate the generous support of AEES for offering a partial award of research scholarship and Smorgon Steel Group for donation of steel tubes.

References

1. Eligenhausen R., Popov E. P., and Bertero V. V. (1983). "Local bond stress-slip relationships of deformed bars under generalized excitations", Report No. UCB/EERC-83/23, Earthquake Engineering Research Center, University of California, Berkeley, California, p102.

2. Gardner A. P. and Goldsworthy H. M. (2004). "Experimental Investigation of the Stiffness of Critical Components in a Moment-resisting Composite Connection", Accepted for publication in the Journal of Constructional Steel Research, 2004.
3. Kankam C. K. (1997). "Relationship of Bond Stress, Steel Stress, and Slip in Reinforced Concrete", Journal of Structural Engineering, ASCE, Vol123, No.1, p79-85.
4. Soroushian P., Obaseki K., Nagi M., and Rojas M. C. (1988). "Pullout Behavior of Hooked Bars in Exterior Beam_Column Connections", ACI Structural Journal, American Concrete Institute, p269-276.
5. Yao H., Goldsworthy H. M., Gad E. F. (2003). "Bond and Anchorage of Cogged Bar within Concrete-filled CHS Column-I Beam Joint", Proceedings of the 2003 Conference, Australian Earthquake Engineering Society.

INCORPORATING UNCERTAINTY IN PROBABILISTIC SEISMIC RISK ANALYSES

ANNETTE PATCHETT, DAVID ROBINSON, TREVOR DHU, AUGUSTO SANABRIA
GEOSCIENCE AUSTRALIA

AUTHORS:

Annette Patchett is a graduate geologist with the Risk Research Group at Geoscience Australia. She is currently investigating models for earthquake risk assessments and uncertainties in risk estimates.

David Robinson is a geophysicist with the Risk Research Group at Geoscience Australia. His main roles include the development of the earthquake hazard model and its application to urban centres around Australia.

Trevor Dhu is a geophysicist with the Risk Research Group of Geoscience Australia. His research is focused on national scale earthquake risk maps as well as developing site response and strong motion models for Australia.

Augusto Sanabria is a risk analyst with the Risk Research Group. His background is in probabilistic modelling, reliability analysis of electrical power systems and risk analysis of fires in buildings. He has an MSc from the University of London and a PhD from Monash University.

ABSTRACT:

Geoscience Australia has developed a model to assess the earthquake risk for Australian communities. A complicated element of earthquake risk assessments lies in the modelling of uncertainties. Probabilistic Seismic Risk Analyses (PSRA) are an effective means of quantifying the effect of these uncertainties. Modelling earthquake risk involves the integration of source, attenuation, site response, building damage and financial loss models.

Incorporating uncertainties in risk estimates is crucial in order to capture the natural variation likely to be encountered during an actual seismic event and to therefore accurately model the associated risk. Two broad categories of uncertainty are associated with PSRA – aleatory uncertainty and epistemic uncertainty. Aleatory uncertainty refers to the unpredictable nature of future events and is modelled using random variables in each PSRA component. It is treated mathematically by sampling the probability density functions (PDFs) associated with each component model. Epistemic uncertainty relates to knowledge limitations and can be associated with variation of the mean and standard deviation of the random variable.

Results from a PSRA conducted solely for residential structures in Newcastle and Lake Macquarie indicate that aleatory uncertainty associated with seismic wave attenuation is more significant than aleatory uncertainty associated with the generation of synthetic earthquakes. Aleatory uncertainty associated with site amplification and building damage is also less significant than aleatory uncertainty associated with seismic wave attenuation and synthetic earthquake generation.

1. INTRODUCTION

Geoscience Australia has developed a model to assess the earthquake risk for Australian communities, a component of which is the appropriate modelling of uncertainties. Given the significant uncertainty surrounding the timing, location and magnitude of future earthquakes, it is necessary to employ a probabilistic seismic risk analysis (PSRA). PSRA can be summarised by the following four primary steps:

1. simulating earthquakes using an earthquake source model;
2. estimating how the level of ground shaking propagates in the bedrock by using the attenuation model;
3. accounting for the local regolith and its affect on ground shaking by incorporating the site response model;
4. estimating the probability of different damage states using the capacity spectrum method and modelling the 'probable' financial loss.

Robinson and Fulford (in press) provide a more detailed description of the methodology.

2. INCORPORATING UNCERTAINTY

Toro *et al.* (1997) introduced a useful way of separating uncertainty into two broad categories:

1. *Aleatory uncertainty:* refers to the natural randomness of a process. Significant parameters of the PSRA are treated as random variables. Each random variable is described by a probability density function (PDF) which describes the probability of a variable taking on a specific value. It has a mean (_) and standard deviation (_). In this paper, aleatory uncertainty is incorporated mathematically by sampling the PDF associated with each random variable to include variation from the mean. Different techniques of sampling the PDF are discussed in detail later in this section.

2. *Epistemic uncertainty:* relates to knowledge limitation and can be associated with uncertainty in a model's ability to adequately describe a process. Mathematically this can be handled by using a range of models with different PDFs. In such cases it is argued that analysing the collection of PDFs provides an improved understanding of the true process. For example, alternative attenuation models are often used in probabilistic seismic hazard analyses (PSHA) and probabilistic seismic risk analyses (Frankel *et al.*, 2000; Adams and Halchuk, 2003).

Aleatory uncertainty and epistemic uncertainty are associated with each of the four primary steps of the PSRA. This paper explores the aleatory uncertainty associated with the source, attenuation, and site response models coupled with the aleatory uncertainty associated with the capacity curve in the capacity spectrum method. The paper also explores different techniques of sampling the PDF when incorporating attenuation uncertainty. Epistemic uncertainty in PSRA has not been considered in this paper. Other studies, however, have indicated that epistemic uncertainty is important when conducting PSRA (e.g. Patchett *et al.* (in press), Robinson *et al.* ASEG 2004).

3. SAMPLING THE PROBABILITY DENSITY FUNCTION

Incorporating aleatory uncertainty involves sampling the PDF of a random variable. The different sampling techniques used for this paper are described briefly below. Robinson and Fulford (in press) provide a more detailed description of the sampling techniques.

1. **Mean:** This technique involves sampling the mean of the PDF.

2. **Random Sampling:** Random sampling involves selecting a single random value from the PDF. In this method a randomly selected value is not weighted against its probability of occurrence. Extremely high or low values, however, have a naturally lower probability of selection. Random sampling incorporates a very low level of spatial correlation. Consequently, a high choice at one location does not correspond with a high choice at other locations (as for low choices).

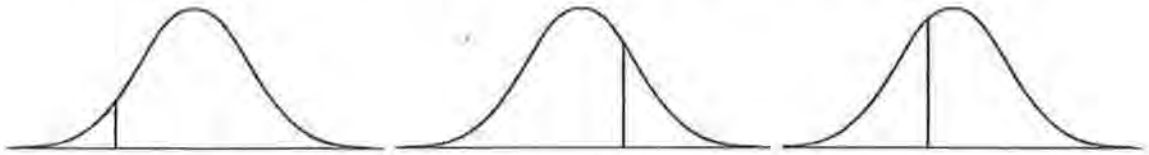

Figure 1 PDFs showing examples of randomly sampled values.

3. **Spawning:** Spawning incorporates an even sampling across the PDF. The PDF is bounded at ±2.5_ and divided into 5 equally spaced bins. A sample is taken at the bin centroid of each bin. Each sample is weighted against its probability of occurrence by evaluating the PDF at the bin centroid and normalising by an appropriate factor. Unlike random sampling, spawning incorporates a high level of spatial correlation. That is a high choice at one location corresponds with a high selection at other locations (as for low choices).

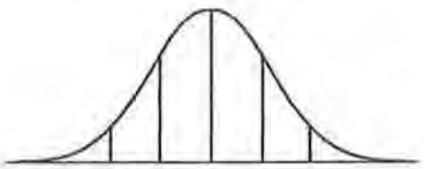

Figure 2 PDF showing 5 spawned values.

4. **Stratified Monte Carlo simulation:** Traditionally the distribution of samples chosen from a PDF via Monte Carlo sampling represents the original PDF. That is, there will be many samples in the vicinity of the mean and fewer samples corresponding to the tails. Stratified Monte Carlo sampling involves taking many samples (typically >1000) from a PDF in a semi-controlled fashion such that the number of samples generated around the mean is roughly the same as the number generated in the tails. The probability of the random variable X equaling each of the sample values also needs to be calculated so that the final simulation results can be weighted against the likelihood of their occurrence.

Robinson and Fulford (in press) discuss the calculation of this probability in detail as well as how it is used to weight the final results of the simulation.

4. *INCORPORATING ALEATORY UNCERTAINTY IN PSRA*

a) **Source Model:** Historical information and geology are used to define earthquake source zones, within which earthquakes of a given magnitude are equally likely to be located. The recurrence of earthquakes in each source zone is described by the bounded cumulative Gutenberg Richter relationship (BCGR) (Kramer, 1996). For any magnitude of interest, the BCGR relationship estimates the number of earthquakes of equal or higher magnitude that are expected in the source zone. A location for each synthetic earthquake is generated by random sampling two uniform PDFs, one describing the latitude range of the source zone and the other describing the longitude range. The orientation of the fault plane for each event is then assigned by using random sampling to take N_s samples from a uniform PDF covering the range -180° to 180°. Each event is assigned a magnitude by using Stratified Monte Carlo sampling with the PDF of the BCGR specific to each source zone. This process ensures that all magnitudes between the minimum magnitude (m_{min}) and the maximum magnitude (m_{max}) are equally represented. Empirical rules are then used to calculate the remaining dimensions of each rupture trace (Robinson and Fulford [in press]).

b) Attenuation Model: Attenuation models describe how the intensity of ground shaking decreases with increasing distance from the earthquake source and defines both the mean and standard deviation of the response spectra (Toro *et al.*, 1997). The Toro *et al.* (1997) attenuation model has been used in this paper because it is believed to be the most appropriate attenuation model that is currently available despite being based on North American data (Dhu *et al*, 2002). Traditional techniques for incorporating attenuation aleatory uncertainty in PSHA typically evaluate the probability of exceeding a certain level of ground motion by integrating underneath the PDF (e.g. Cornell, 1968; Kramer, 1996). Such techniques are not compatible with the Capacity Spectrum Method (see below) and as such the mean, random sampling and spawning techniques are all used to incorporate aleatory uncertainty associated with the attenuation model.

c) Site Response Model: The Newcastle study area has been divided into 6 distinct site classes, within which the regolith is assumed homogeneous. The amplification factors in each site class are represented by a PDF that describes the transfer of earthquake motion from the unweathered bedrock to the ground surface (Dhu *et al*, 2002). In this paper the mean, spawning and random sampling techniques are all used to incorporate aleatory uncertainty associated with the amplification model.

d) Capacity Spectrum Method and Financial Model: The standard capacity spectrum method is used to estimate the damage to buildings. The vertical position of the capacity curve ultimate point is assumed to follow a log-normal probability density function with standard deviation of 0.3 (FEMA, 1999). The mean and

random sampling techniques are used to select the ultimate point and hence capacity curve for each building – synthetic earthquake combination.

5. *CASE STUDY: NEWCASTLE AND LAKE MACQUARIE*

A PSRA has been conducted solely for residential structures in the Newcastle and Lake Macquarie region to highlight the effect of aleatory uncertainty. The region's seismicity was classified into 3 source zones; the Newcastle Triangle Zone (NTZ), Newcastle Fault Zone (NFZ) and the Tasman Sea Margin Zone (TSMZ) (Dhu *et al.*, 2002). We generated approximately 1200 earthquakes for each synthetic earthquake catalogue (500 in NTZ, 300 in NFZ, and 400 in each of TSMZ).

Figure 3 illustrates the probable maximum loss (PML) curves obtained when the three different sampling techniques are used to incorporate attenuation aleatory uncertainty. Each of the lines with the same colour and style corresponds to a different synthetic earthquake catalogue produced with the sampling techniques described above. Variations within the same line colour and style are indicative of the uncertainty associated specifically with the generation of each synthetic earthquake catalogue. Note that for the results in Figure 3, the mean sampling technique was used with the amplification and capacity curve models. Figure 4 illustrates the effect on the PML curves when incorporating aleatory uncertainty (using random sampling) in the amplification factor and capacity curve respectively, when random sampling is used to incorporate aleatory uncertainty for attenuation.

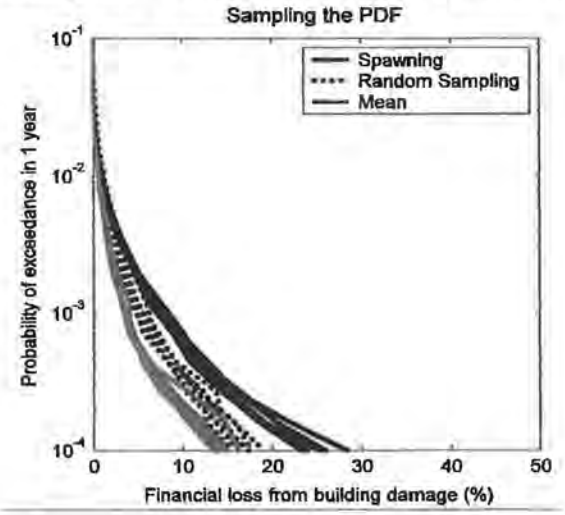

Figure 3 Effect of using different sampling techniques to incorporate aleatory uncertainty in attenuation (using the Toro et al., (1997) attenuation model).

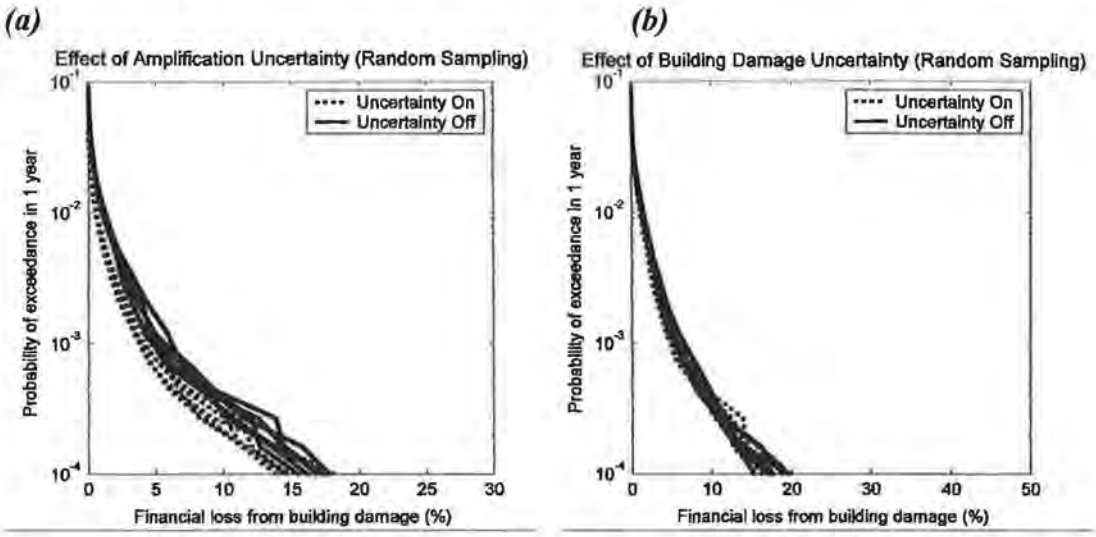

Figure 4 Effect of aleatory uncertainty with the (a) amplification and (b) building damage models; when aleatory uncertainty for attenuation is incorporated with random sampling.

6. DISCUSSION

PSRA encompass a number of associated aleatory uncertainties, each exerting a different level of influence on risk estimates. Figures 3 and 4 demonstrate that aleatory uncertainty associated with attenuation exerts a greater influence on risk than all other aleatory uncertainty in PSRA. This is shown by the significant difference between risk estimated using each of the three sampling techniques. Aleatory uncertainty associated with the synthetic earthquake generation is of secondary significance, and this is in turn greater than aleatory uncertainty associated with building damage and amplification (Figure 4).

The results presented herein demonstrate that **different techniques** for incorporating aleatory uncertainty associated with attenuation produce highly varying results. Using the mean sample from the attenuation model consistently produces the lowest PML compared with random sampling and spawning. This is because both random sampling and spawning incorporate selections of attenuation greater than the mean, and hence this is reflected in the resultant estimated risk. In nature, however, a consistent mean level of ground shaking will not occur at all sites. Random sampling and spawning are therefore considered the two key sampling methods for incorporating aleatory uncertainty in attenuation.

Figure 3 illustrates that random sampling produces marginally higher estimates of loss for high probability/low risk events. For low probability/high risk events, however, spawning estimates significantly higher loss than random sampling. This difference between random sampling and spawning is largely associated with the difference in the level of spatial correlation associated with the two techniques. When using spawning, the same generated ground motion is correlated across all building sites, i.e. a high choice at one location corresponds with a high choice at all other locations. In random sampling, however, a high choice at one location does not correspond with a high

choice at other locations, and as such individual ground motions are site specific. In the PML this is highlighted because the loss values expressed represent the loss to the study region (i.e. an aggregate of loss for all buildings).

REFERENCES

Adams, J., and Halchuk, S. (2003) Fourth generation seismic hazard maps of Canada: Values for over 650 Canadian localities intended for the 2005 National Building Code of Canada, Geological Survey of Canada Open File 4459, pp 155.

Cornell, C.A. (1968) Engineering seismic risk analysis, Bulletin of the Seismological Society of America, Vol 58, pp 1583-1606.

Dhu, T., and Jones, T. (2002) Earthquake risk in Newcastle and Lake Macquarie: ACT, Geoscience Australia, GA Record 2002/15.

Dhu, T., Robinson, D., Sinadinovski, C., Jones, T., Corby, N., Jones, A., Schneider, J. (2002) Earthquake Hazard, Chapter 4 in Earthquake risk in Newcastle and Lake Macquarie: ACT, Geoscience Australia, GA Record 2002/15, pp 43-76.

FEMA (1999), HAZUS Technical Manual. National Institute of Building Science: Federal Emergency Management Agency.

Frankel, A.D, Mueller, C.S., Barnhard, T.P., Leyendecker, E.V., Wesson, R.L., Harmsen, S.C., Klein, F.W., Perkins, D.M., Dickman, N.C., Hanson, S.L., and Hopper, M.G. (2000) USGS National Seismic Hazard Maps, Earthquake Spectra, Vol 16.

Kramer, S. L. (1996) Geotechnical Earthquake Engineering. Prentice Hall, New Jersey.

Patchett, A.M., Robinson, D.J., Dhu, T. Investigating earthquake risk models and uncertainty in probabilistic seismic risk analyses. ACT, Geoscience Australia (in press)

Robinson, D., and Fulford, G. EQRM: Earthquake Risk Modelling Software Technical Manual, Version 2.0. ACT, Geoscience Australia (in press)

Robinson, D., Mendez, A., Fulford, G., Dhu, T., Jones, T., and Schneider, J., (2003) Recent advances in the modelling of earthquake hazard in Australia: part 2 – estimating the hazard: ASEG 16th Geophysical Conference and Exhibition, February 2003, Adelaide.

Toro, G.R., Abrahamson, N.A., and Schneider, J.F. (1997) Model of strong ground motions from earthquakes in Central and Eastern North America: best estimates and uncertainties, Seismological Research Letters, Vol 68, pp 41-57.

DESIGN EARTHQUAKE GROUND MOTION PREDICTION AND SIMULATION FOR PMA BASED ON A MODIFIED ENA SEISMIC GROUND MOTION MODEL FOR SWWA

HONG HAO[1], BRIAN GAULL[2]

[1]SCHOOL OF CIVIL AND RESOURCE ENGINEERING, THE UNIVERSITY OF WESTERN AUSTRALIA
35 STIRLING HIGHWAY, CRAWLEY, WA 6009, AUSTRALIA

[2]GURIA CONSULTING, P.O. BOX A122, AUSTRALIND, WESTERN AUSTRALIA

AUTHORS:

Hong Hao is a professor of structural dynamics in the School of Civil and Resource Engineering, the University of Western Australia. He received his PhD degree in Department of Civil Engineering, University of California at Berkeley. Before joining UWA in 2002, he worked as a post-doc researcher in Seismographic Station in UC Berkeley and was an associate professor in Nanyang Technological University in Singapore. His research interests are structural dynamics, earthquake and blast engineering.

Brian A Gaull is director of Guria Consulting. He has been interested in Seismic Hazard and Strong Ground Motion since his first appointment with GA (formerly BMR) over 30 years ago. Two decades of such experience enabled him to set up Guria Consulting in Western Australia more then 13 years ago.

ABSTRACT

A Probabilistic Seismic Hazard Analysis (PSHA) was carried out for rock sites in the Perth Metropolitan Area (PMA). This entailed the derivation of magnitude recurrence relations for three source zones in the southwest of Western Australia (SWWA) and for the background seismicity. Using these relations and an attenuation function derived for Central and Eastern United States (CEUS) as input, the PGA of 475-year event was estimated to be about 0.09 g. Deaggregation was then used to estimate which magnitude was the most likely to produce this event. This result however, was found to be very sensitive to the adopted b-Value. Hence, because of inherent uncertainties in this parameter, two design events corresponding to likely extreme b-Values were chosen. They were ML6.9 at a distance of 62 km and ML5.6 at a distance of 21 km. A worst-case scenario event of ML7.5 distance 50 km was also determined. Ground motion time histories on rock site and on two soft soil sites in PMA corresponding to these three events were simulated and their response spectra calculated. The response spectra are compared with the respective design spectra given in the current Australian earthquake code for PMA. Discussions on the adequacy of the design spectra are made.

Design Earthquake Ground Motion Prediction and Simulation for PMA Based on a Modified ENA Seismic Ground Motion Model for SWWA

Hong Hao[1], Brian Gaull[2]

[1]School of Civil and Resource Engineering, the University of Western Australia

35 Stirling Highway, Crawley, WA 6009, Australia

[2]Guria Consulting, P.O. Box A122, Australind, Western Australia

ABSTRACT

A Probabilistic Seismic Hazard Analysis (PSHA) was carried out for rock sites in the Perth Metropolitan Area (PMA). This entailed the derivation of magnitude recurrence relations for three source zones in the southwest of Western Australia (SWWA) and for the background seismicity. Using these relations and an attenuation function derived for Central and Eastern United States (CEUS) as input, the PGA of 475-year event was estimated to be about 0.09 g. Deaggregation was then used to estimate which magnitude was the most likely to produce this event. This result however, was found to be very sensitive to the adopted b-Value. Hence, because of inherent uncertainties in this parameter, two design events corresponding to likely extreme b-Values were chosen. They were ML6.9 at a distance of 62 km and ML5.6 at a distance of 21 km. A worst-case scenario event of ML7.5 distance 50 km was also determined. Ground motion time histories on rock site and on two soft soil sites in PMA corresponding to these three events were simulated and their response spectra calculated. The response spectra are compared with the respective design spectra given in the current Australian earthquake code for PMA. Discussions on the adequacy of the design spectra are made.

1. PSHA

A PSHA was carried out for a rock site in downtown Perth. The source zone configuration is shown in Figure 1. Magnitude recurrence in these three zones and background seismicity was evaluated after aftershocks and foreshocks were removed. The adopted Gutenburg-Richter A and b-Values for these zones are given in Table 1.

Table 1
ML Recurrence parameters for seismic zones

SZ	A	b
1	2.88	0.75
2	4.22	1.27
3	3.1	0.85
Background	0.021(ML4)	0.81

Fig. 1 Seismic zones around PMA and the corresponding ML recurrence parameters

The attenuation relation used in the PSHA is based on CEUS data (Toro et al, 1997) which is expressed in terms of moment magnitude (Mw). It is acknowledged that the

magnitude conversion used for the SWWA database (predominantly the Richter Scale, or ML) and Mw is not universal and may introduce significant differences, should other conversions be used. Using a standard deviation of 0.7 for the attenuation and other inputs as described above, the 475-year design event for rock sites in Perth was estimated to be about 0.09 g. This is consistent with the AS1170.4 (1993) and Dhu et al (2004).

There is clearly any number of combinations of magnitude and distance that could satisfy the design PGA. However, it is usual to find the particular combination that is most likely to produce the design PGA event of interest. In order to do this a process known as "deaggregation" is used as described hereunder.

2. DEAGGREGATION

The magnitude sub-intervals selected in this process, as well as the probabilistic contribution from each, is displayed in Figure 2. It can be seen that the PGA event for repeat times of less than 100 years (say PGA < 0.04 g) is driven predominantly by events of ML6 +/- 0.5 as these events have the greatest risk per annum in this PGA range. In the same way, the 475-year event (PGA ~ 0.09 g) is driven by events in the upper ML range (ML6.6-7.5). However, because the frequency of earthquakes of ML7 (or more) decreases about 4-fold when the b-Value increases from 0.75 to 1.0, if the mid-magnitude event frequency remains unchanged, the contribution to the hazard from this upper ML range diminishes accordingly. The effect of increasing the b-Values for both SZ1 and the Background seismicity to unity is shown in Figure 3. It is seen that the smaller magnitude events now contribute most and large magnitudes the least for the PGA events of interest. Furthermore, if a b-Value of 0.9 is adopted, the contributions from all ML sub-intervals converge and are about equal. What this shows is how critical the adopted b-Value is in determining the ML of the most likely design event.

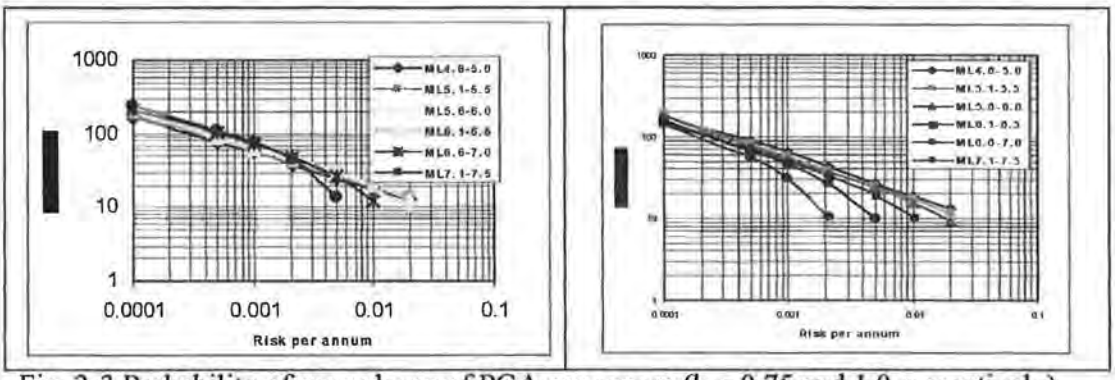

Fig. 2-3 Probability of exceedance of PGA per annum (b = 0.75 and 1.0 respectively)

The range of adopted b-Value in recent studies indicates the uncertainty of this critical parameter: e.g. Gaull and Michael-Leiba (1987) obtained 0.90 for SZ1; Dhu et al (2004) used 1.0 for all zones and the value of 0.75 was obtained for this paper. The reason for the variation between the first and last result is due to the difference of method used in curve fitting as well as the time intervals used to determine lower magnitude recurrence rates. Dhu et al (2004) assume a b-Value of 1, because it is the world average. It is because of this uncertainty in b-Value for the SWWA, that two events have been selected.

As can be seen in Figure 2 a typical ML for the 475-year design event is in the range 6.5<ML<7.6. Consequently, a Meckering sized ML6.9 (Mw7.0) event has been chosen to be representative of this. Using Toro et al (1997) a mean distance of 62 km gives rise to a typical PGA for the 475-year event. This distance corresponds with that between the city and the western side of SZ1, where this event is most likely to occur.

Similarly from Figure 3, an ML5.6 event is mid-range of the sub-interval with the greatest contribution. Using Toro attenuation, the corresponding mean distance required to produce 0.09 g at a rock site is about 21 km. Hence, this event could arise from either the background seismicity or possibly on the western edge of SZ2.

3. WORST-CASE SCENARIO EVENT

Gaull and Michael-Leiba (1987) performed a seismic risk analysis for SWWA and predicted that the maximum earthquake for the seismic zone 1 is ML7.5. As shown in Figure 1, the shortest distance from seismic zone 1 to PMA is 50 km. This is considered as the worst-case scenario event for PMA in this study.

4. GROUND MOTION SIMULATION

Ground motion time histories on rock site at PMA corresponding to the above three events are stochastically simulated. Each simulated time history is compatible with the ground motion spectrum of the modified ENA ground motion model for SWWA (Hao and Gaull 2004). Four simulations are carried out for each case. More detailed discussion on the modified ground motion model for SWWA and ground motion simulation can be found in (Hao and Gaull 2004). Figure 4 shows a typical simulated ground motion time history and comparison of its Fourier spectrum with the model spectrum.

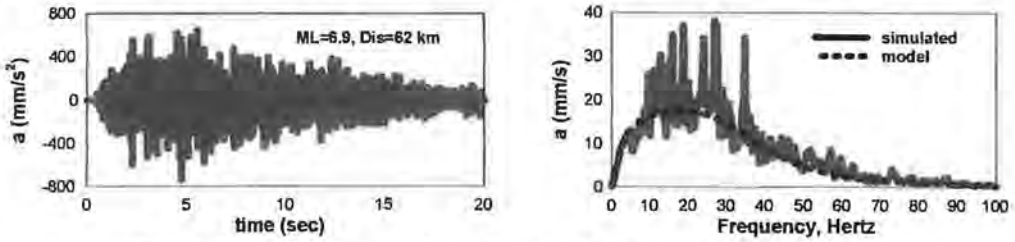

Fig. 4 Simulated ground motion time history on rock site in PMA

Two soft soil sites, as shown in Figure 5, in PMA are used to study the site amplification effects on seismic waves. The simulated rock motions are assumed consisting of SH-wave and used as input to the site. The incident angle is assumed as 60°. The soil nonlinearity is modelled using the nonlinear soil properties suggested by Seed and Idriss (1970) and accounted for in site response calculation (Hao 1993).

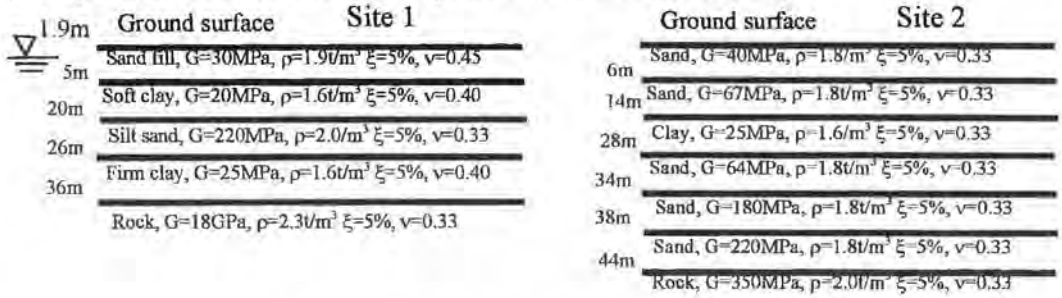

Fig. 5 Soft soil sites in PMA used in the study

Site 1 has the average S-wave velocity=152.5m/s, average P-wave velocity=356.2m/s, and the fundamental horizontal soil profile frequency=1.06Hz, vertical frequency=2.47Hz. Site 2 has the average S-wave velocity=195.4m/s, average P-wave velocity=387.9m/s, and the fundamental horizontal soil profile frequency=1.11Hz, vertical frequency=2.20Hz. Figure 6 shows the calculated surface ground motion time histories and their Fourier spectra at the two sites corresponding to the base rock motion

shown in Figure 4. As shown both sites amplify ground motion at low frequencies (less than 3Hz) corresponding to the site natural vibration frequencies, but deamplify ground motions at frequencies higher than 3 Hz. This is more clearly seen on pseudo velocity response spectra illustrated in Figure 7. As shown, although the two design events give rise to very similar PGA values, the upper range design event results in larger velocity and displacement values. The two sites deamplify ground motion in the acceleration range, but amplify velocity and displacement at frequencies lower than 3 Hz. Table 2 lists the average PGA and PGV values obtained from the four simulations of ground motions.

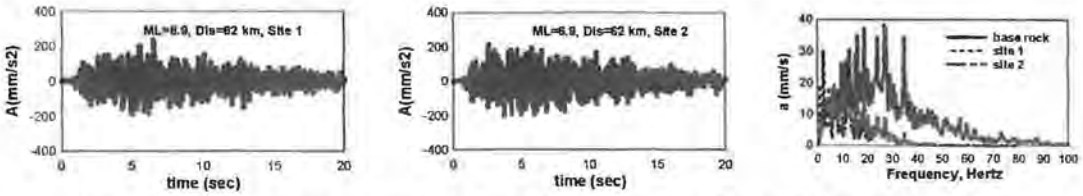

Fig. 6 Calculated ground motion time histories on surface of the two soil sites

Table 2 Peak ground motion values

Site	ML=7.5, D=50 km		ML=6.9, D=62 km		ML=5.6, D=21 km	
	PGA(mm/s^2)	PGV(mm/s)	PGA(mm/s^2)	PGV(mm/s)	PGA(mm/s^2)	PGV(mm/s)
Rock	1845	24.01	702	9.64	424	3.69
Site1	595	36.50	225	9.79	100	2.69
Site2	740	23.45	289	8.57	132	2.57

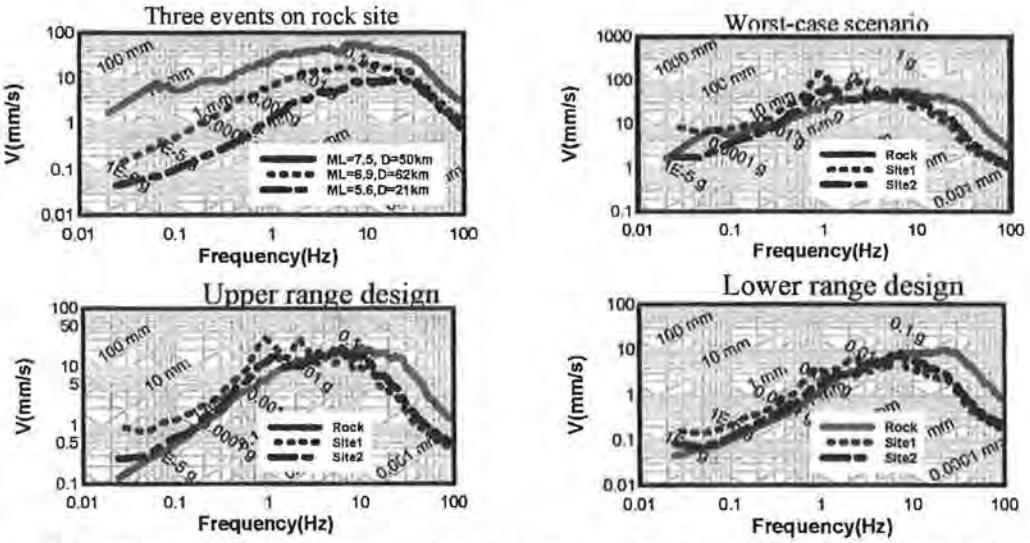

Fig. 7 Comparison of pseudo velocity response spectra of the estimated ground motions

Figure 8 compares spectral acceleration of the simulated ground motions with the code design spectrum for PMA. As shown, the code provided spectral acceleration values are adequate for the two soil sites, even for the worst-case scenario earthquake, because these sites are relatively soft and deamplification of ground acceleration occurs. However, they are inadequate for the rock site during the worst-case scenario event. It should be noted that the observations made above are based on the assumption that the design event will generate PGA value of 0.09g on rock site in PMA and considered only two soft soil sites. Should a different design event be determined from the seismicity study, (eg by choosing a different attenuation relation), and/or a relatively harder site is analysed, different conclusions may be derived.

5. CONCLUSIONS

From the seismicity study, two 475-year return period design events for PMA were determined. The two events represent upper and lower range design events. Ground motions on rock and two soft soil sites in the PMA corresponding to the two design events and a worst-case scenario event for the PMA, are simulated. Because of the relatively high frequency contents of the ground motions on rock site, the soft soil sites deamplify ground motion acceleration, but amplify ground velocity and displacement at frequencies less than 3 Hz. The design spectra in the current Australian code overestimate spectral accelerations on soft soil sites from the three events, but greatly underestimate spectral accelerations of the ground motion on rock site corresponding to the worst-case scenario event in the period range of less than 0.2 sec.

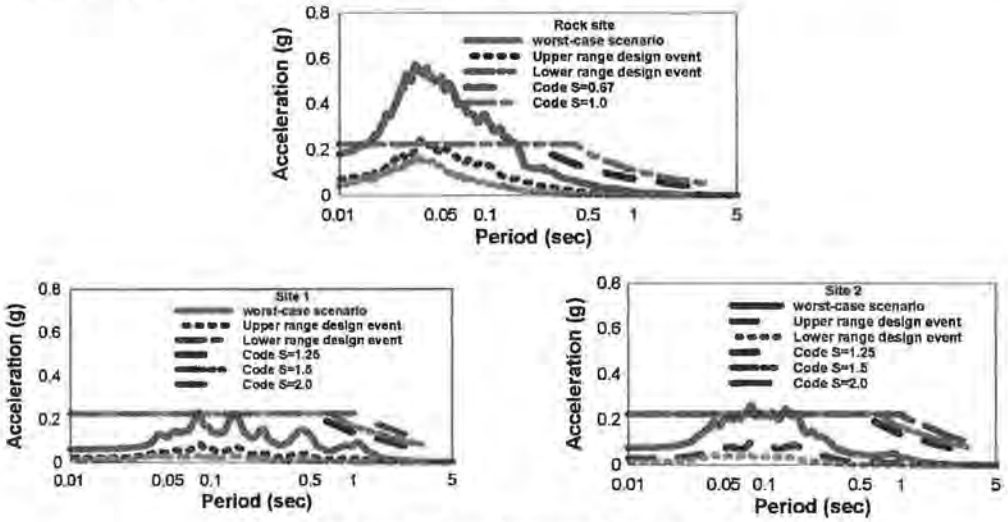

Fig. 8 Comparison of spectral accelerations

REFERENCES

Dhu, T., Sinadinovski, C., Edwards, M., Robinson, D., Jones T. and Jones, A. (2004) Earthquake risk assessment for Perth, Western Australia. Proceedings of the 13Th World Conference on Earthquake Engineering, August 2004, Vancouver, Canada.

Gaull, B. and Michael-Leiba, M. (1987) Probabilistic earthquake risk maps of southest Western Australia, BMR Journal of Australian Geology and Geophysics, Vol. 10, pp145-151.

Hao, H. (1993) Input seismic motions for use in structural response analysis, Soil Dynamics and Earthquake Engineering, VI, Editor A. S. Cakmak and C. A. Brebbia, Elsevier Applied Science, pp87-100.

Hao, H. and Gaull, B. (2004) Prediction of Seismic Ground Motion in Perth Western Australia for Engineering Application, Paper No. 1892, Proceedings of the 13Th World Conference on Earthquake Engineering, August 2004, Vancouver, Canada.

Seed, H. B. and Idriss, I. M. (1970) Soil moduli and damping factors for dynamic response analysis, Report No. UCB/EERC-70-10, Earthquake Engineering Research Center, University of California at Berkeley.

Standards Australia (1993)Australian Standard: Minimum design loads on structures, Part 4: Earthquake loads – AS1170.4 – 1993'

Toro, G. R., Abrahamson N. A. and Schneider J. F. (1997) Model of strong ground motions from earthquakes in central and eastern United States. Seismological Research Letters, Vol. 68(1); 41-57.